AGU PUBLICATIONS

Tectonics

RESEARCH ARTICLE
10.1002/2017TC004491

Special Section:
Orogenic cycles: from field observations to global geodynamics

Episodic behavior of Gondwanide deformation in eastern Australia: Insights from the Gympie Terrane

Derek Hoy[1] and Gideon Rosenbaum[1]

[1]School of Earth and Environmental Sciences, University of Queensland, Brisbane, Queensland, Australia

Abstract The mechanisms that drove Permian-Triassic orogenesis in Australia and throughout the Cordilleran-type Gondwanan margin is a subject of debate. Here we present field-based results on the structural evolution of the Gympie Terrane (eastern Australia), with the aim of evaluating its possible role in triggering widespread orogenesis. We document several deformation events (D_1–D_3) in the Gympie Terrane and show that the earliest deformation, D_1, occurred only during the final pulse of orogenesis (235–230 Ma) within the broader Gondwanide Orogeny. In addition, we found no evidence for a crustal suture, suggesting that terrane accretion was not the main mechanism behind deformation. Rather, the similar spatiotemporal evolution of Permian-Triassic orogenic belts in Australia, Antarctica, South Africa, and South America suggest that the Gondwanide Orogeny was more likely linked to large-scale tectonic processes such as plate reorganization. In the context of previous work, our results highlight a number of spatial and temporal variations in pulses of deformation in eastern Australia, suggesting that shorter cycles of deformation occurred at a regional scale within the broader episode of the Gondwanide Orogeny. Similarly to the Cenozoic evolution of the central and southern Andes, we suggest that plate coupling and orogenic cycles in the Late Paleozoic to Early Mesozoic Gondwanide Orogeny have resulted from the superposition of mechanisms acting at a range of scales, perhaps contributing to the observed variations in the intensity, timing, and duration of deformation phases within the orogenic belt.

Key Points:
- Major deformation in Gympie Terrane occurred during the final episode of Hunter-Bowen Orogeny in southeast Gondwana
- Lack of a suture, an Australian origin, and the structural evolution of the Gympie Terrane do not support arc collision-driven orogenesis
- Both plate reorganization and local plate coupling variations likely affected episodic Gondwanide deformation at differing length scales

Supporting Information:
- Supporting Information S1

Correspondence to:
D. Hoy,
d.hoy1@uq.edu.au

Citation:
Hoy, D., and G. Rosenbaum (2017), Episodic behavior of Gondwanide deformation in eastern Australia: Insights from the Gympie Terrane, *Tectonics*, *36*, 1497–1520, doi:10.1002/2017TC004491.

Received 25 JAN 2017
Accepted 20 JUN 2017
Accepted article online 3 JUL 2017
Published online 10 AUG 2017

1. Introduction

Orogenic cycles are commonly attributed to episodes of enhanced plate coupling intermitted by periods of tectonic relaxation and/or crustal extension [*Beltrando et al*., 2007; *Collins*, 2002; *Lister et al*., 2001]. In accretionary orogens, such episodes may be triggered by local changes in the subduction dynamics that were associated with, for example, terrane accretion [*Huang et al*., 2000] or the arrival of anomalously thick oceanic crust at the subduction zone [*Cloos*, 1993; *Lallemand et al*., 1992; *Rosenbaum and Mo*, 2011]. Alternatively, enhanced coupling may correspond to global tectonic plate reorganization events [e.g., *Silver et al*., 1998] that may trigger a cascade of plate tectonic changes. Such orogenic processes play a fundamentally important role in the tectonic evolution of continents, and their recognition is therefore crucial for understanding and reconstruction of past tectonic events.

The Pacific/Iapetus margin of Gondwana (cf. Terra Australis Orogen) has been affected by intense orogenesis from the Late Paleozoic to Early Mesozoic (~300–230 Ma) in what is known as the Gondwanide Orogeny [*Cawood*, 2005; *Du Toit*, 1937; *Veevers and Morgan*, 2000]. Enhanced coupling has been linked to accretion of exotic terranes, particularly along the West Gondwana part of the orogen [*Vaughan and Pankhurst*, 2008]. However, it has also been suggested that enhanced coupling was driven by increased convergence rates following a plate reorganization event [*Cawood*, 2005]. In the Australian sector of the Gondwanan margin, orogenesis mostly occurred in association with repeated cycles of subduction zone advance and retreat [Collins, 2002], and although exotic terranes have been suggested to play a role, there is some disagreement with regard to the autochthonous or allocthonous origin of some suspected exotic terranes, including the Gympie Terrane (e.g., *Aitchison and Buckman* [2012] versus *Li et al*. [2015]). Whether the Gondwanide orogenesis in the Australian segment, locally known as the Hunter-Bowen Orogeny, has resulted from large-scale plate kinematic changes [*Cawood and Buchan*, 2007] or from local features within the subduction zone [*Buckman et al*., 2015; *Jenkins et al*., 2002; *Korsch et al*., 2009b; *Li et al*., 2012; *Nutman et al*., 2013] is still an open question.

The Permian-Triassic Gympie Terrane is located in eastern Australia (Figure 1) and was originally thought to be an anomalous tectonic association that did not fit the predicted distribution of more widespread orogenic rocks [*Day et al*., 1978]. Correlations with terranes in New Zealand and New Caledonia, on the basis of

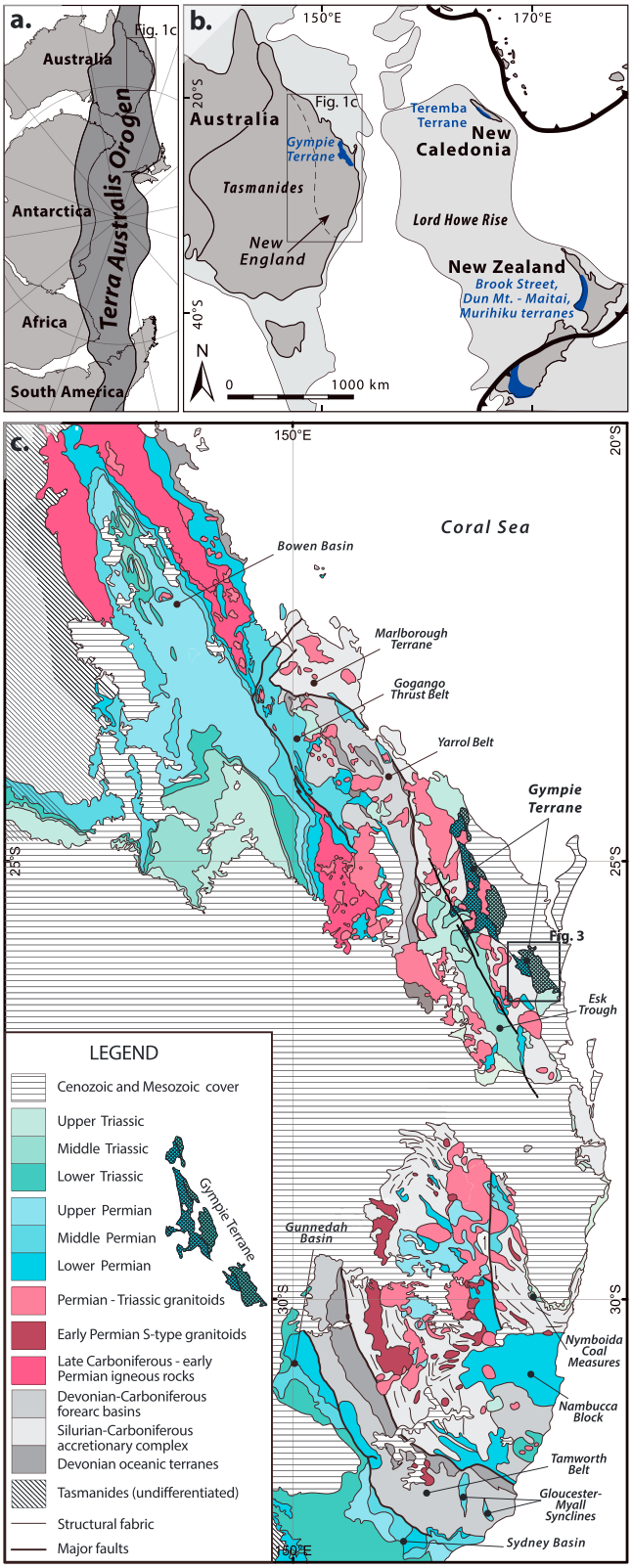

Figure 1. (a) Late Paleozoic configuration of Gondwana [*Domeier and Torsvik*, 2014] showing the approximate extent of the Terra Australis Orogen. Latitude and longitude grid spacing is 30°; (b) crustal elements of Australia and peri-Gondwanan terranes of the SW Pacific [after *Collot et al.*, 2012]. Gympie Terrane and suggested correlatives highlighted in blue; (c) simplified geological map of eastern Australia (data from Geoscience Australia).

geochemical and petrographic similarities [*Harrington*, 1974; *Sivell and Waterhouse*, 1988; *Waterhouse and Sivell*, 1987], were interpreted to suggest that a laterally extensive exotic island arc terrane had been accreted to the Gondwanan margin [*Cawood*, 1984; *Korsch et al*., 2009b; *Waterhouse and Sivell*, 1987]. Accordingly, it has been suggested that the Hunter-Bowen Orogeny was directly linked to the accretion of an exotic island arc [*Buckman et al*., 2015; *Harrington and Korsch*, 1985; *Nutman et al*., 2013]. Geochemical and detrital zircon data, however, do not support this interpretation, suggesting that the Gympie Terrane did not originate far from the Australian continental crust [*Korsch et al*., 2009c; *Li et al*., 2015; *Sivell and McCulloch*, 2001]. Whether the Gympie Terrane is completely autochthonous, as suggested by *Li et al.* [2015], or paraautochthonous with respect to eastern Australia, has remained unresolved. However, there is only limited information available regarding the deformation history of the Gympie Terrane, which remains a major impairment in assessing the origin of the terrane and its relationship with the Hunter-Bowen Orogeny. The Gympie Terrane therefore presents an opportunity to test the mechanisms that drove cycles of deformation in the Gondwanide Orogeny.

This paper presents new field-based data on the style of deformation in the Gympie Terrane. These new structural data are complemented by a synthesis of existing structural and geochronological constraints on Hunter-Bowen deformation. The results provide insights into the episodic nature of deformation in an ancient cordilleran-type accretionary orogen, with specific implications for the fundamental controls on plate coupling along the active Gondwanan margin during the Late Paleozoic to Early Mesozoic.

2. Geological Setting

The Terra Australis Orogen formed at the paleo-Pacific margin of Gondwana and can be traced along the margin from Australia to South America (Figure 1a) [*Cawood*, 2005]. It consists of a Neoproterozoic rift and passive continental margin assemblage and a succession of Paleozoic convergent plate margin assemblages that are well preserved in the Tasmanides of eastern Australia (Figure 1b) [*Cawood*, 2005; *Glen*, 2013]. The youngest and most easterly assemblage in the Tasmanides (New England, Figures 1b and 1c) mainly consists of the following: (1) Devonian to Carboniferous subduction-related rocks, (2) Early Permian rift-related rock units, and (3) middle Permian to Late Triassic continental arc-related rocks that formed simultaneously with Hunter-Bowen Orogeny [*Day et al*., 1978; *Holcombe et al*., 1997a, 1997b; *Korsch et al*., 2009a; *Murray et al*., 1987]. The Hunter-Bowen Orogeny is mainly recognized in three main periods of contractional deformation: an initial ~270–260 Ma phase of deformation (HBO 1), renewed ~253 Ma deformation and rapid foreland loading (HBO 2), and a final ~235–230 Ma phase of deformation (HBO 3) [*Holcombe et al*., 1997b]. At the continental scale, Hunter-Bowen Orogeny transformed the New England zone into a doubly vergent fold belt [*Holcombe et al*., 1997b]. Hunter-Bowen crustal loading led to increased subsidence and the formation of an ~1600 km long retroforeland basin to the west, in the Permian-Triassic Bowen, Gunnedah, and Sydney basins (Figure 1c) [*Korsch and Totterdell*, 2009]. The underlying cause (or causes) of these periods of increased plate coupling is not well understood, with many different models proposed including flat-slab subduction [*Jenkins et al*., 2002; *Korsch et al*., 2009b; *Li et al*., 2012], increased convergence following plate reorganization [*Cawood and Buchan*, 2007], or the accretion of a suspect oceanic arc comprising the Gympie Terrane and its now-dispersed along-strike correlatives (Figure 1b) [*Buckman et al*., 2015; *Cawood*, 1984; *Korsch et al*., 2009b; *Nutman et al*., 2013; *Waterhouse and Sivell*, 1987].

The Gympie Terrane is situated in eastern Australia, in the central part of the New England zone, and is separated by a tectonic contact from Devonian-Carboniferous accretionary complex rocks to the west (Figures 1b and 1c). However, the nature of this tectonic contact and its kinematics is poorly understood. Some authors contend that the Gympie Terrane is an exotic terrane with island arc geochemical affinities [*Sivell and Waterhouse*, 1988] with the tectonic contact possibly representing a crustal suture zone. Alternatively, the Gympie Terrane may have developed at or near the eastern margin of the Australian plate as an arc fore-arc assemblage [*Sivell and McCulloch*, 2001; *Li et al*., 2015] that was either autochthonous or paraautochthonous. If so, the tectonic contact may only represent a fault associated with the Permian-Triassic Hunter-Bowen Orogeny and/or younger wrench reactivation [e.g., *Babaahmadi and Rosenbaum*, 2014a, 2014b]. In any case, $^{40}Ar/^{39}Ar$—biotite cooling ages of 237 ± 0.4 Ma to 234 ± 0.4 Ma [*Tang*, 2004] on stitching plutons suggest that the terrane was adjacent to the New England accretionary complex before the end of the Hunter-Bowen Orogeny in the Late Triassic.

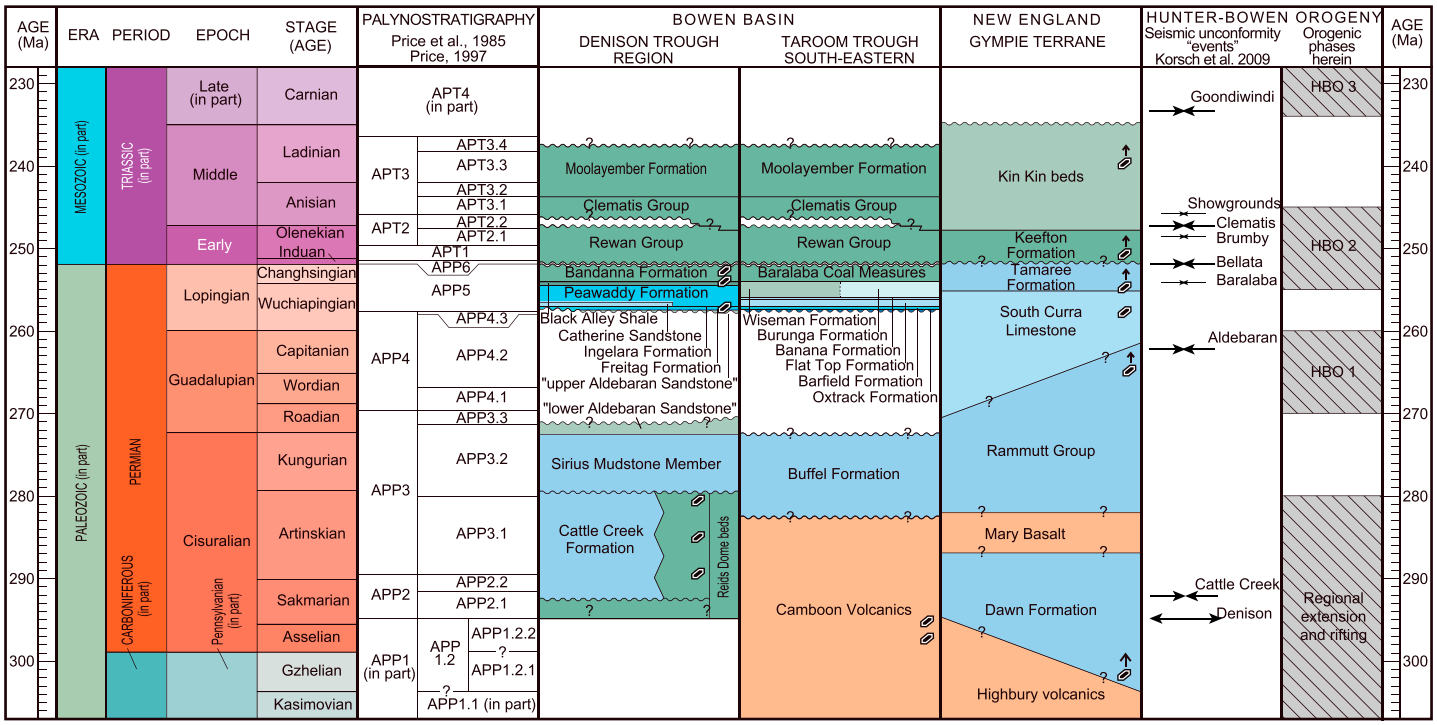

Figure 2. Stratigraphic framework of the Gympie Terrane and coeval foreland basin. Stratigraphic units of the Gympie Terrane [after *Stidolph et al.*, 2016] with age control based on fossils [*Runnegar and Ferguson*, 1969; *Waterhouse and Balfe*, 1987] and U-Pb zircon geochronology [*Li et al.*, 2015]. Seismic unconformities of *Korsch et al.* [2009b] are adjusted to a recalibrated Bowen Basin stratigraphy and timescale [*Nicoll et al.*, 2015; *Laurie et al.*, 2016].

Geochemical and Sm/Nd isotope studies [*Sivell and Waterhouse*, 1988; *Sivell and McCulloch*, 2001] suggest that the Gympie Terrane formed in a convergent plate margin setting, with tholeiitic basalts in the lowermost unit sourced from a depleted asthenospheric mantle source that was metasomatized by hydrous fluids from the subducted lithosphere [*Sivell and McCulloch*, 2001]. While this process could represent juvenile oceanic-arc magmatism, the overlying dacitic rocks formed as products of extensive melt fractionation [*Sivell and Waterhouse*, 1988; *Sivell and McCulloch*, 2001], which suggests a more mature arc setting. The overlying intermediate volcanic rocks are dominant and are thought to require the incorporation of a substantial amount of continental-derived greywackes into the melts [*Sivell and McCulloch*, 2001], thus further supporting the idea that the Gympie Terrane did not originate as a typical juvenile intraoceanic arc.

Rocks in the Gympie Terrane are predominantly marine extrusive and pyroclastic volcanic rocks, as well as volcanogenic sedimentary rocks (Figure 2) [*Arnold*, 1996; *Cranfield*, 1999; *Murphy et al.*, 1976; *Runnegar and Ferguson*, 1969; *Waterhouse and Balfe*, 1987; *Stidolph et al.*, 2016]. The lower part of the succession is dominated by basaltic to dacitic volcanic and deep marine sedimentary rocks of the Highbury, Mary, and Dawn formations. The depositional environment shallows upward into volcanogenic sandstone and conglomerate with subordinate andesitic volcanic and volcaniclastic rocks, followed by impure limestone (Rammutt Group and South Curra Limestone). These rocks are overlain by rhythmically interbedded marine sandstones and siltstones of the Tamaree Formation, which are in turn unconformably overlain by terrestrial conglomerate and coarse sandstone of the Keefton Formation. The Kin Kin beds are the uppermost unit in the Gympie Terrane, comprising a tectonically thickened sequence of slate, shale, cleaved sandstone, and phyllite that dominates the eastern part of the terrane.

Regional mapping shows that a number of fault systems dissect the Gympie Terrane into a mosaic of blocks [*Cranfield*, 1999], which are most apparent in the Permian rocks within and surrounding the Gympie Goldfield (Figure 3). The Gympie Terrane records at least two phases of contraction and thrust faulting; early contraction folded the succession and generated a slaty cleavage in the central and eastern part of the terrane, while later contraction involved, for example, a bedding subparallel postmineralization décollement that cuts the cleaved country rock and synmineralization magmatic rocks, truncating the top of the Gympie ore body at

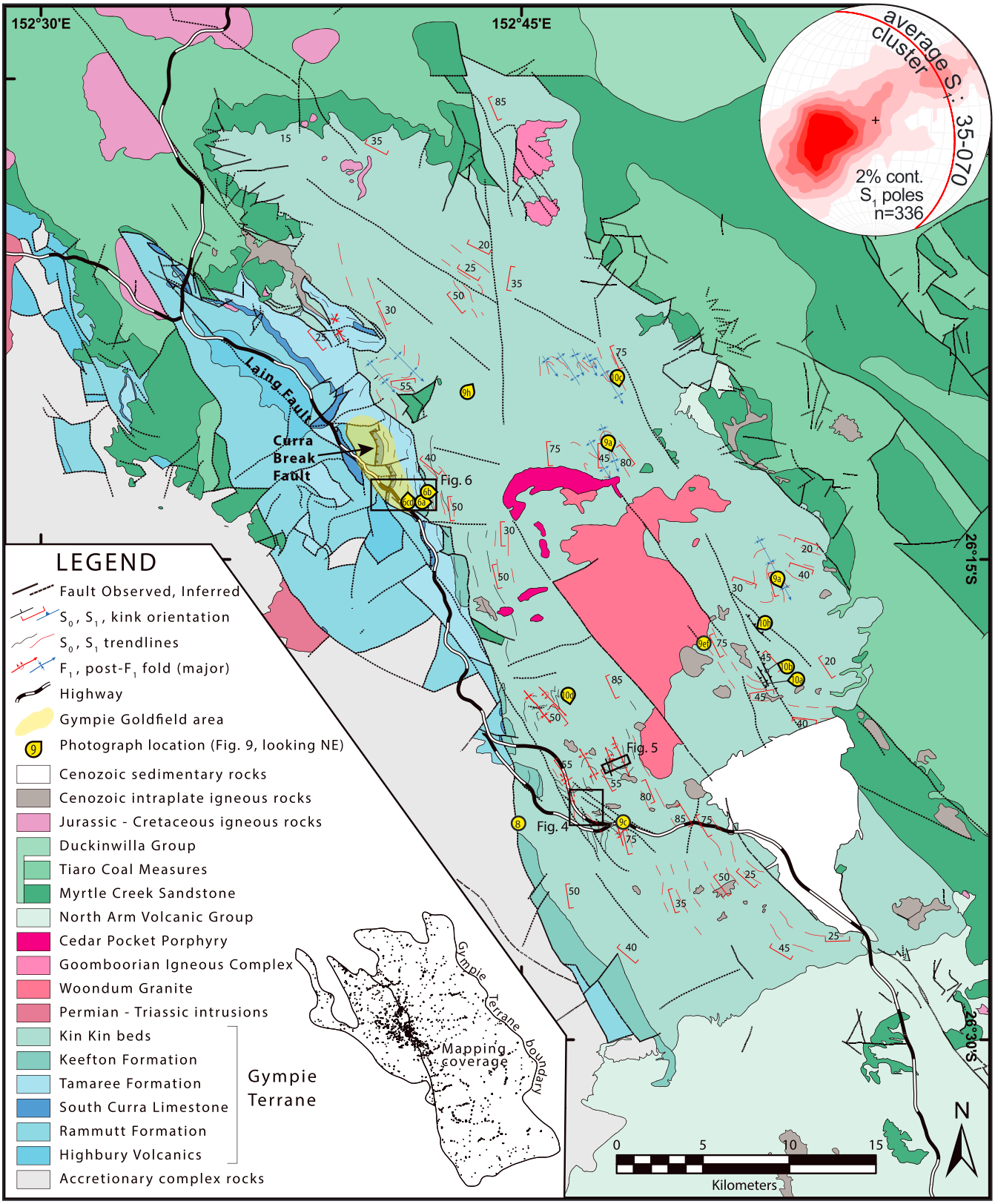

Figure 3. Map showing solid geology and structure of the Gympie Terrane. Modified and revised from *Cranfield* [1999] based on field observations and interpretation of tilt angle-filtered aeromagnetic data (line spacing 50 m, data from Geological Survey of Queensland). Note that the labeled yellow markers correspond to field photograph locations and are oriented to show the view direction.

the base of the South Curra Limestone (Curra Break Fault, Figure 3) [*Arnold*, 1996; *Crawford*, 2003; *Stidolph et al*., 2016]. Late stage E-W striking normal faults are present, as well as late NW-NNW striking strike-slip faults such as the Laing Fault [*Arnold*, 1996; *Cranfield*, 1999; *Matthai et al*., 1991; *Stidolph et al*., 2016], which is a major structure in the Gympie Terrane and one of many NNW striking faults throughout eastern Australia. Although early reverse movement is suggested by the juxtaposition of Lower Permian against Upper Permian rocks in map view (Figure 3), the dominant motion on the fault is related to late-stage reactivation with predominantly sinistral strike-slip kinematics [*Stidolph et al*., 2016], possibly during Mesozoic and/or Cenozoic wrenching [e.g., *Babaahmadi and Rosenbaum*, 2014a, 2014b].

3. Methods

We collected structural and lithological observations ($n \approx 1200$) from 700 field sites in the Gympie Terrane (see mapping coverage inset in Figure 3). These were complemented by observations from existing maps produced by the Geological Survey of Queensland ($n \approx 2400$) and Gympie Eldorado Gold Mine ($n \approx 1500$). To understand the overall structure of each outcrop, we measured the orientation of structures using a geological compass and documented the local lithology, fabric intensity, deformation style, crosscutting relationships, overprinting criteria, and kinematic indicators. Most outcrops showed evidence for one or more phases of deformation that were each characterized on the basis of the deformation style and overprinting relationships to determine the local structural history at each outcrop (see section 4). Throughout the terrane, we correlated the different structural features on the basis of their distinct deformation style and recognized a consistent pattern in the relative timing of structures. This information was then used to construct a regional deformation history for the Gympie Terrane (section 5). Note that the location of all insets and field photographs appear in the relevant map figures as black boxes and yellow circles, respectively.

4. Structural Observations From the Gympie Terrane

A number of major road cuttings provide excellent exposures of the Kin Kin beds that clearly demonstrate structural and overprinting relationships of deformation and intrusive rocks in the southern Gympie Terrane (Figure 4a). Bedding planes (S_0) are commonly preserved as thin sandstone beds or interlaminations, and a strong slaty cleavage (S_1) is ubiquitous. The S_1 cleavage orientation changes at each outcrop (Figures 4b–4h) indicating a polyphase deformation history. Moderately inclined, overturned F_1 folds are observed at the small (~10^1 m) scale and are evident at outcrop (>10^2 m) scale from bedding cleavage relationships, changes in fold vergence, and structural facing (Figure 4i). Folds are noncylindrical and four structural domains (Figures 4e–4h) are present within the area of the cross section (Figure 4i). A series of 2–60 m (commonly 6–7 m) thick mafic to intermediate dykes and a 15–20 m thick felsic dyke are observed in outcrop (Figures 4a and 4f), coinciding with anomalies in tilt angle-filtered magnetic data. The dykes are steeply dipping and strike NW to NNW and are observed to cut the S_1 slaty cleavage at a low angle and thus were intruded after S_1. Minor faults cut both the S_1 slaty cleavage and dykes (Figure 4j), as do small kink bands and large kink folds, which refold the first generation folds and strongly influence the S_1 orientation (Figures 4b–4f). Some kink-style folds appear to have formed at the tips of faults, similar in style to fault propagation folds (Figure 4j), whereas others are unrelated to faulting. Kinematic indicators from some NE dipping faults, such as Riedel shears, asymmetrical strain shadows around resistant clasts, asymmetrical foliation, and dragging of the S_1 cleavage, provide evidence that brittle style reactivation involved normal kinematics (Figure 4k) that postdated a more ductile phase of reverse movement preserved in the hanging wall rocks adjacent to the fault (Figure 4l). The normal-sense offset of kink folds intersecting the NE dipping faults (Figures 4i and 4m) indicate that normal faulting postdates the kink folds.

The relationship between first-generation overturned folds and the penetrative slaty cleavage is demonstrated in an E-W transect along Coles Creek Road (Figure 5). In this region, S_0 has been folded parallel to the S_1 axial planar cleavage to form kilometer-scale F_1 folds that are steeply inclined, overturned, and plunge moderately toward the north (Figures 5a and 5b). The dominant S_1 cleavage dips steeply toward the ENE and is a continuous foliation defined by the alignment of fine white and brown mica, pressure dissolution seams, and strain shadows around sand-sized particles. S_0 is commonly clearly defined by thin sandy layers or volcanogenic interlaminations (Figures 5c and 5d), which appear as a characteristic lithology in the southern

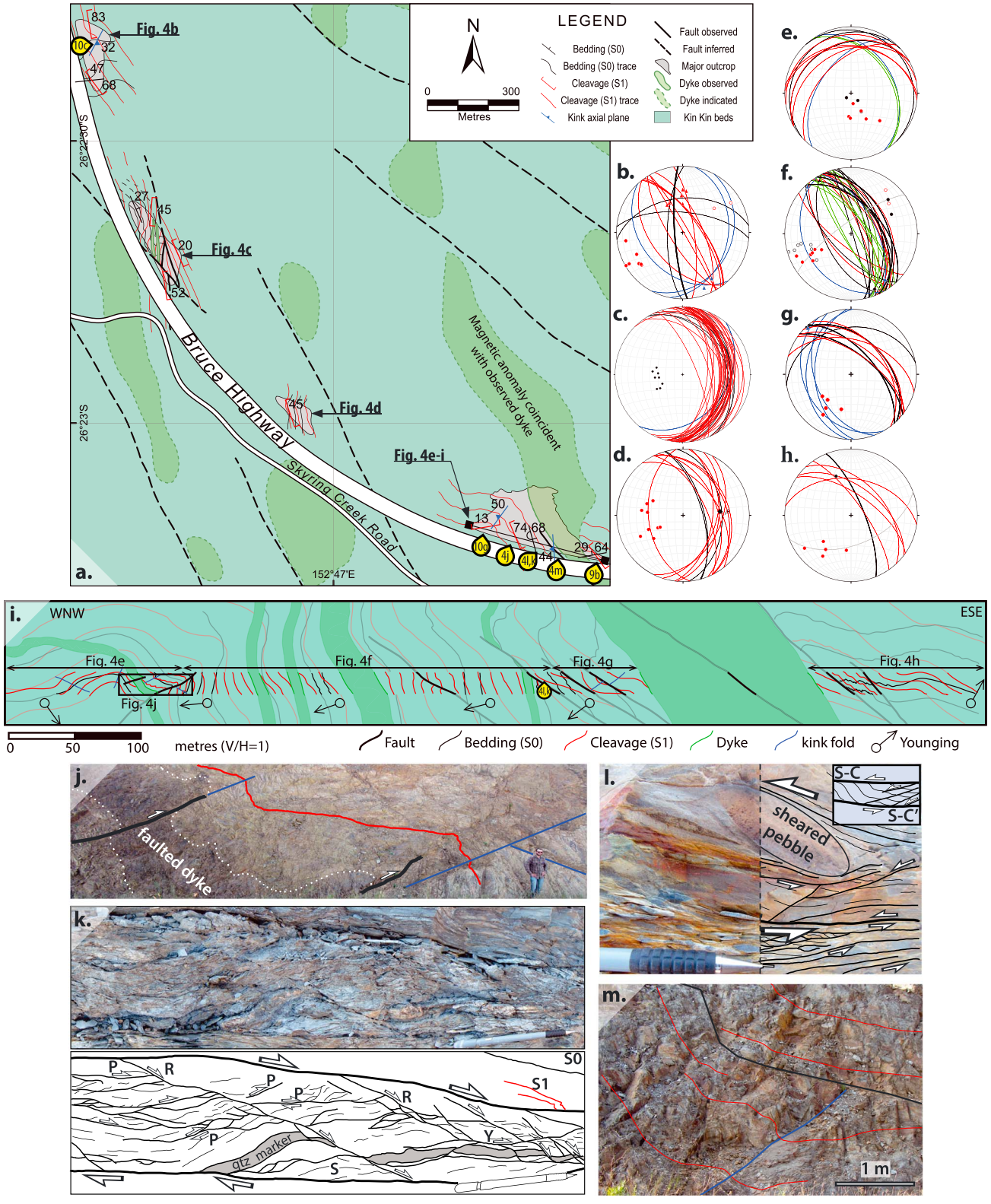

Figure 4. (a) Structural map of the southern Kin Kin beds. See Figure 3 for location; (b–h) equal-area projections for structural domains highlighted in map and cross section. Lines (measured planes), circles (poles, open are overturned), and triangles (fold hinges) are color coded to represent S_0 (black), S_1 (red), kink folds (blue), and dykes (green); (i) cross section with faults (thick black lines) and reconstructed F_1 folds (greyscale); (j) SW dipping thrusts (black) and kink folds (blue) with accommodation faults; (k) foliated cataclastite in fault core showing S-C′ fabrics and asymmetric boudinage indicating normal kinematics; (l) asymmetric strain cap and shadow around clast in hanging wall of fault indicate reverse kinematics; and (m) fault cutting kink fold axial plane.

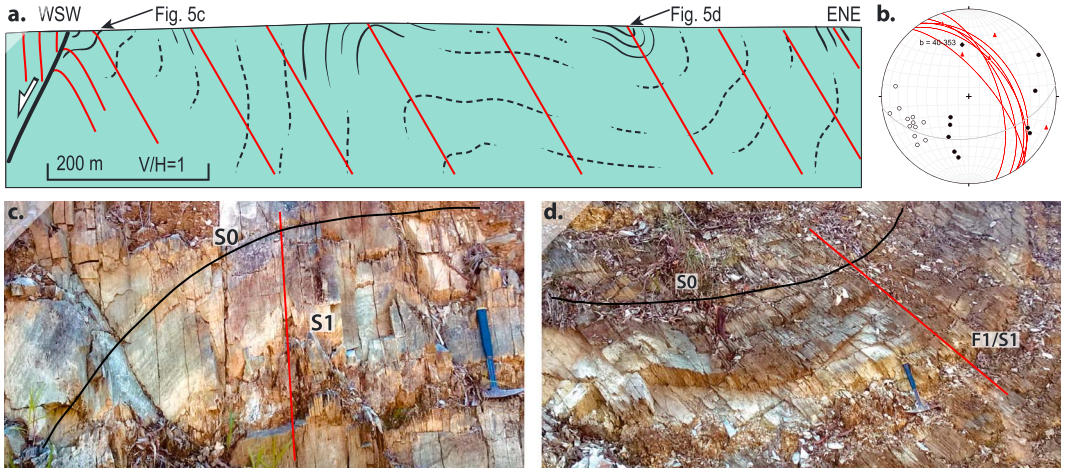

Figure 5. (a) Cross section of overturned F_1 folding within the Kin Kin beds along Coles Creek Road. See Figure 3 for location; (b) stereoplot showing poles to S_0 (black circles normal younging and open circles reverse younging), S_1 planes (red stroke), L_{10} intersection lineation (red triangles), and calculated beta axis (black diamond); (c) steepening S_0 and spaced S_1 cleavage in F_1 anticline; and (d) hinge of F_1 synform.

part of the Kin Kin beds. S_0 is steeper than S_1 in the forelimb, suggesting that the rocks are structurally overturned with vergence toward the west. The backlimb is not overturned and dips moderately ENE.

The southern part of the Gympie Goldfield has a complex structure related to several phases of deformation, each with a distinct structural style. In this area, rocks from all stratigraphic levels form an approximately homoclinal sequence that dips moderately toward the east. A first generation (S_1) cleavage is consistently recognized in both Permian and Triassic rocks throughout most of the area (Figure 6a). The intensity of the S_1 cleavage ranges from millimeter spacing in psammites and volcanic rocks to completely penetrative in pelites, and we also recognize an increase in S_1 intensity toward the contact with the Triassic rocks to the east. Near this contact, we observed bands of protomylonite displaying downdip stretching lineations and reverse kinematics (Figure 6b), which are interpreted as a fault contact that cuts across both bedding and the S_1 cleavage between the Permian Tamaree Formation and Triassic Keefton Formation (Figure 6b, see Figures 3 and 6e for location). Farther west, we observed an east dipping fault, subparallel to bedding, within weakly cleaved rocks of the Tamaree Formation at the intrusive contact with a weathered dyke (Figures 6c and 6d). Subsidiary faults parallel to the main fault displace the intrusive contact with reverse kinematics (Figure 6c), suggesting early reverse movement on the fault, while dragging of early-formed structures and an oblique foliation in the main fault core (Figure 6d) suggest that this fault was reactivated with normal kinematics. While we did not observe the Curra Break Fault, other workers [*Arnold*, 1996; *Crawford*, 2003] have documented a similar two-phase history for the Curra Break Fault (Figure 6e). The Laing Fault is the youngest structure in this area and dips steeply toward the ENE (Figure 6e).

In the northwestern part of the study area, excellent exposures of the South Curra Limestone and part of the Rammutt Group occur in a large quarry (Figure 7a). Bedding is steeply dipping to the NE and structural overturning of the succession is supported by both a young zircon age from the structurally lowermost rocks (258.3 ± 2.6 Ma) [*Li et al.*, 2015] and an inverted faunal succession [*Runnegar and Ferguson*, 1969]. Overturning may also be supported by the vergence of minor recumbent folds nearby (Figures 7b and 7d), although they could also be related to dragging and reverse movement on the numerous bedding-parallel faults (Figures 7a and 7d). Regardless of the origin of the folds, the overturned succession is cut by two shallowly NE dipping thrusts (Figures 7a and 7c) that display steeply pitching slickenlines and congruous fracture steps (Figure 7e), indicating reverse kinematics. These structures are in turn cut by several bedding-subparallel normal faults, which are recognized from the slight truncation of bedding as well as the development of 5–50 cm fault breccia zones. A weak to moderate asymmetrical cleavage is commonly observed in or near these fault surfaces (Figure 7f) and may be interpreted as either dragging of a preexisting S_1 foliation or as a localized fault-related fabric. In either case, the geometric relationship with the adjacent faults indicates normal kinematics. The youngest deformation recognized in this location was a subvertical, NW striking fault

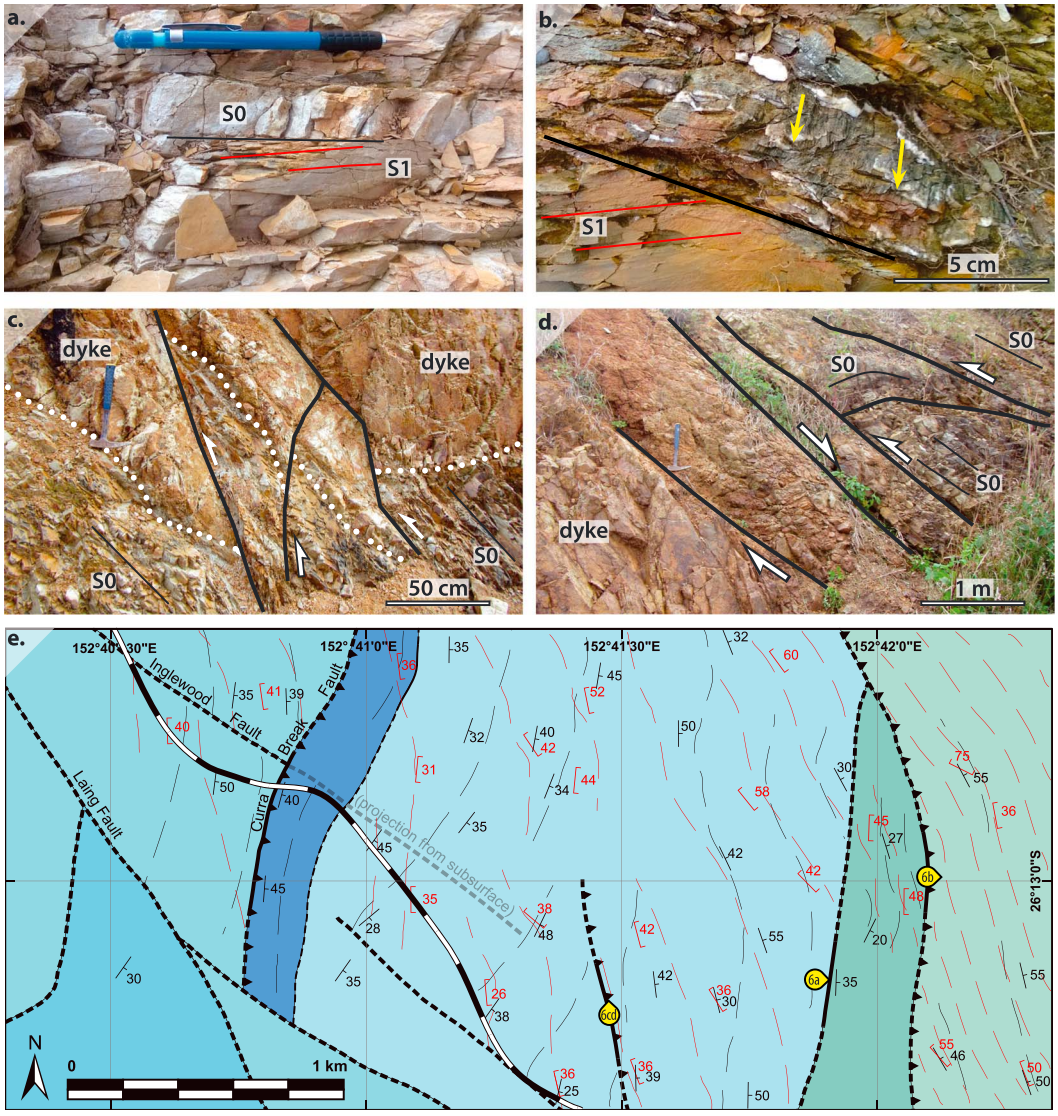

Figure 6. Key observations from the southern Gympie Goldfield. See Figure 3 for location. (a) Main foliation in Tamaree Formation, S_1, is slightly steeper than S_0; (b) zone of thin protomylonite bands with steeply pitching stretching lineation (yellow arrows) marks the fault contact between Tamaree and Keefton formations; (c) intrusive contact between dyke and Tamaree Formation (dotted line) offset by minor reverse faults in footwall of main fault (Figure 6d); and (d) main fault immediately to the east of Figure 6c. Faults preserved in the hanging wall define a small duplex, and local dragging of S_0 suggests reverse kinematics, but well-developed dragging and lensoid structures in the footwall damage zone suggest significant normal movement; (e) structural map of the southern Gympie Goldfield (legend as per Figure 3). Note that the spacing of S_1 form lines represents the intensity of the fabric.

that cuts the earlier structures and juxtaposes the overturned South Curra Limestone in the quarry pit against shallowly dipping South Curra Limestone and Rammutt Group to the east. Disparate bedding attitudes on either side of the fault zone suggest that the offset on this fault is relatively major. The sheared fault rock contains blocks of coal with tuffaceous partings, which may correlate with the Lower Jurassic Tiaro Coal Measures from the unconformably overlying Maryborough Basin (Figure 3).

In the south of the Gympie Terrane, we observed the Triassic Kin Kin beds and Keefton Formation juxtaposed against the Paleozoic accretionary complex rocks by a tectonic contact (Figure 8, see marker in Figure 3 for location). The fault contact strikes N-S with a subvertical dip, and rocks in this area display a steeply dipping macroscopic scaly fabric that suggest predominantly dextral kinematics (Figures 8a and 8b). At the micro-scale, rarely preserved dextral kinematic indicators such as S-C fabrics and en-échelon gash veins are over-printed by brittle-ductile deformation with sinistral kinematics in association with carbonate and Fe-oxide

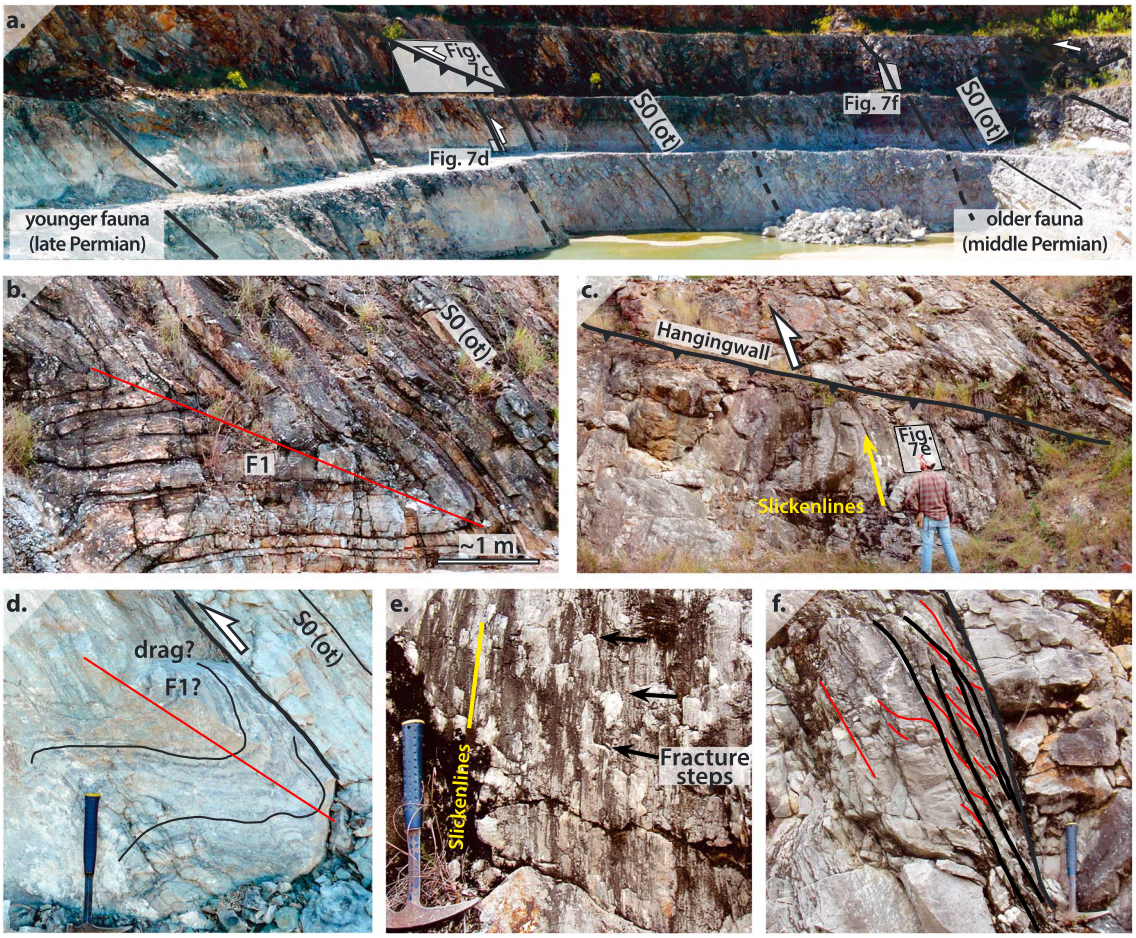

Figure 7. (a) Panoramic photograph (looking NW) of overturned strata in the South Curra Limestone with many bedding-subparallel faults (thick black lines). Quarry pit dimensions are ~100 m × 200 m. See Figure 3 for location; (b) overturned fold cut by minor bedding-parallel fault; (c) shallow fault with well-developed slickensides displaying steps and striations indicating reverse kinematics. Arrows show movement direction of the hanging wall; (d) minor recumbent fold in footwall of fault indicates dragging during reverse kinematics or recumbent fold cut by bedding-parallel fault; and (e) close-up of footwall slickenside from Figure 7c. Steeply pitching slickenlines and congruous fracture steps indicate reverse kinematics; (f) steep fault subparallel to S_0. Footwall rocks are slightly more pelitic and have a poorly developed S1 cleavage that is parallel to the axial plane of recumbent folds (Figures 7b and 7d).

alteration (Figures 8c and 8d). Reactivated zones are distinguishable by the occurrence of red Fe-(hydr)oxide-rich fault breccia and cataclasite that overprints the foliated country rock. The sinistral reactivation appears to have been localized on discrete subvertical N-S striking fault surfaces that are parallel to, and within, the larger dextral fault zone.

5. Structural Interpretation

5.1. First Deformation (D_1)

S_1 is the dominant tectonic fabric that was recognized in the Permian to Triassic rocks of the Gympie Terrane. The S_1 foliation is recognized as a penetrative slaty or phyllitic cleavage. At the mesoscale, the spacing of S_1 changes in response to lithology from continuous in pelites (Figure 9a) to mm to cm scale in psammites (Figure 9b). Microscopically, S_1 is defined by the alignment of fine mica grains, elongation of quartz grains, pressure shadows around resistant clasts, and pressure dissolution seams (Figure 9c). S_1 is also recognized as an axial planar cleavage (Figure 9d) associated with west vergent macroscopic and mesoscopic F_1 folds that range from tight to isoclinal and asymmetrical to overturned. F_1 folds are steeply to shallowly inclined with gently plunging hinges. Based on the consistent orientation of S_1 in areas where D_2 and D_3 are less intense, and the orientation of F_3^1 kink fold hinges farther to the east, the original orientation of S_1 is thought to dip moderately toward the ENE.

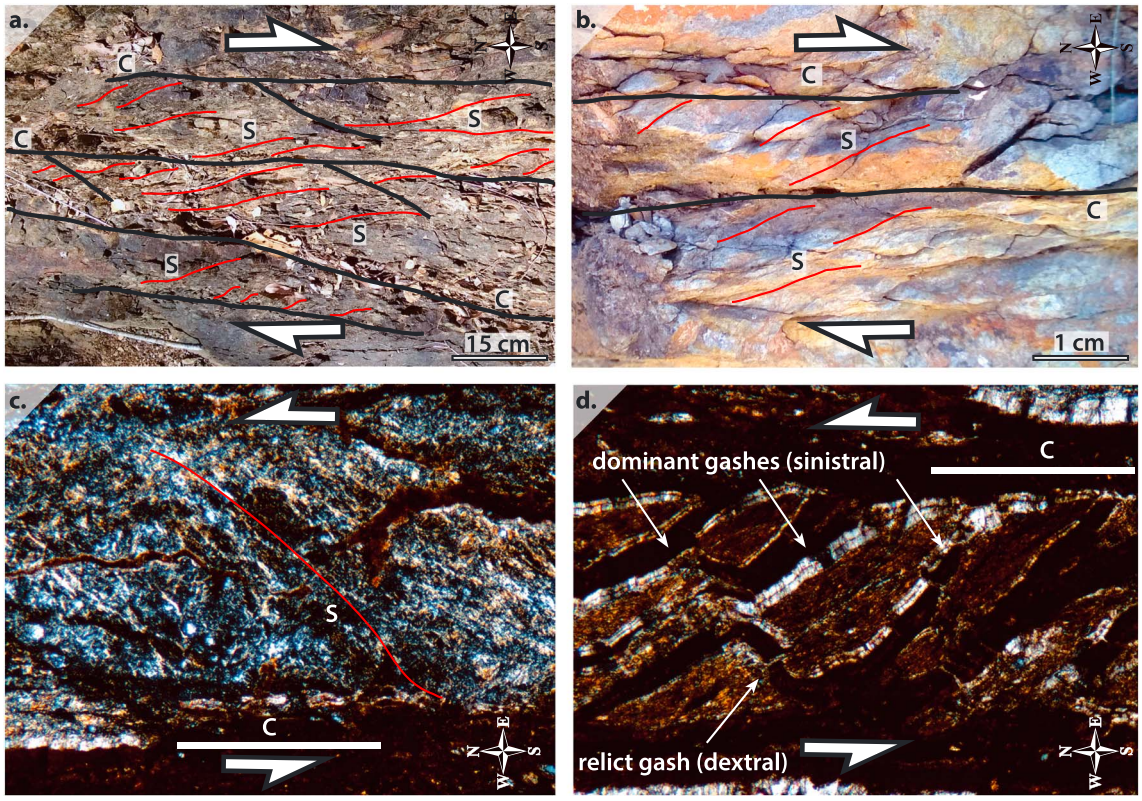

Figure 8. Tectonic contact between Gympie Terrane and D'Aguilar Block. (a, b) Map view photographs show a predominantly dextral component of deformation in the damage zone of the terrane bounding fault. See Figure 3 for location; (c, d) map view photomicrographs of oriented sample 1 m from Figure 8b show evidence for fault reactivation with opposing kinematics. While dextral kinematic indicators such as en-échelon gash veins and S-C fabrics are only rarely preserved in this part of the fault zone (Figure 8d), they are clearly overprinted by carbonate and Fe-oxide alteration as well as brittle-ductile deformation associated with sinistral kinematics, as constrained by incipient S-C fabrics (Figure 8c) and en-échelon gash veins (Figure 8d).

The spatial distribution and intensity of D_1 deformation is heterogeneous within the Gympie Terrane, with a strain gradient that increases toward the contact with the Triassic rocks to the east (cf. section 6.1 and Figure 6e). S_1 cleavage and F_1 folds appear to be less well developed or entirely absent from some volcanic and sedimentary rocks of the western part of the terrane. Within the Gympie Goldfield, Permian rocks situated between the Laing Fault and Triassic rocks to the east (Figures 3 and 7) are weakly cleaved in the west, ranging to moderately dipping and moderately cleaved in the east. A zone of more intense D_1 deformation occurs in siltstone, slate, and phyllite of the Kin Kin beds farther the east (Figures 3 and 7), where large-scale overturned F_1 folds and ubiquitous S_1 cleavage are evident. The abrupt boundary between the moderately dipping and moderately cleaved rocks and the intensely deformed Triassic rocks to the east was observed to be a post-D_1 fault in one locality (Figure 6b). Although this boundary was not directly observed in other areas, we can place it between outcrops near the edge of the Kin Kin beds in several places throughout the southern part of the terrane, which we interpret as a fault.

Constraints on the timing of D_1 deformation are obtained from hornfelsed slate that is developed adjacent to intrusive contacts with the Woondum Granite (Figure 3). This rock shows evidence for contact metamorphism that has affected the foliated Kin Kin beds, resulting in the authigenic growth of cordierite poikiloblasts containing S_1 inclusion trails (Figures 9e and 9f). The presence of S_1 mica inclusions, together with the lack of D_1 strain shadows around the cordierite, suggests that D_1 deformation occurred prior to intrusion. Other evidence of magmatism following D_1 deformation includes the presence of one or more swarms of crosscutting dykes that intrude at a low angle to the S_1 fabric of the Kin Kin beds (Figures 9g and 9h). The dykes cut the S_1 cleavage locally faulted and/or folded (Figure 9h). In many places these intrusions are associated with localized fine-scale kinking within the aureole that seems unrelated to the deformation phases outlined herein.

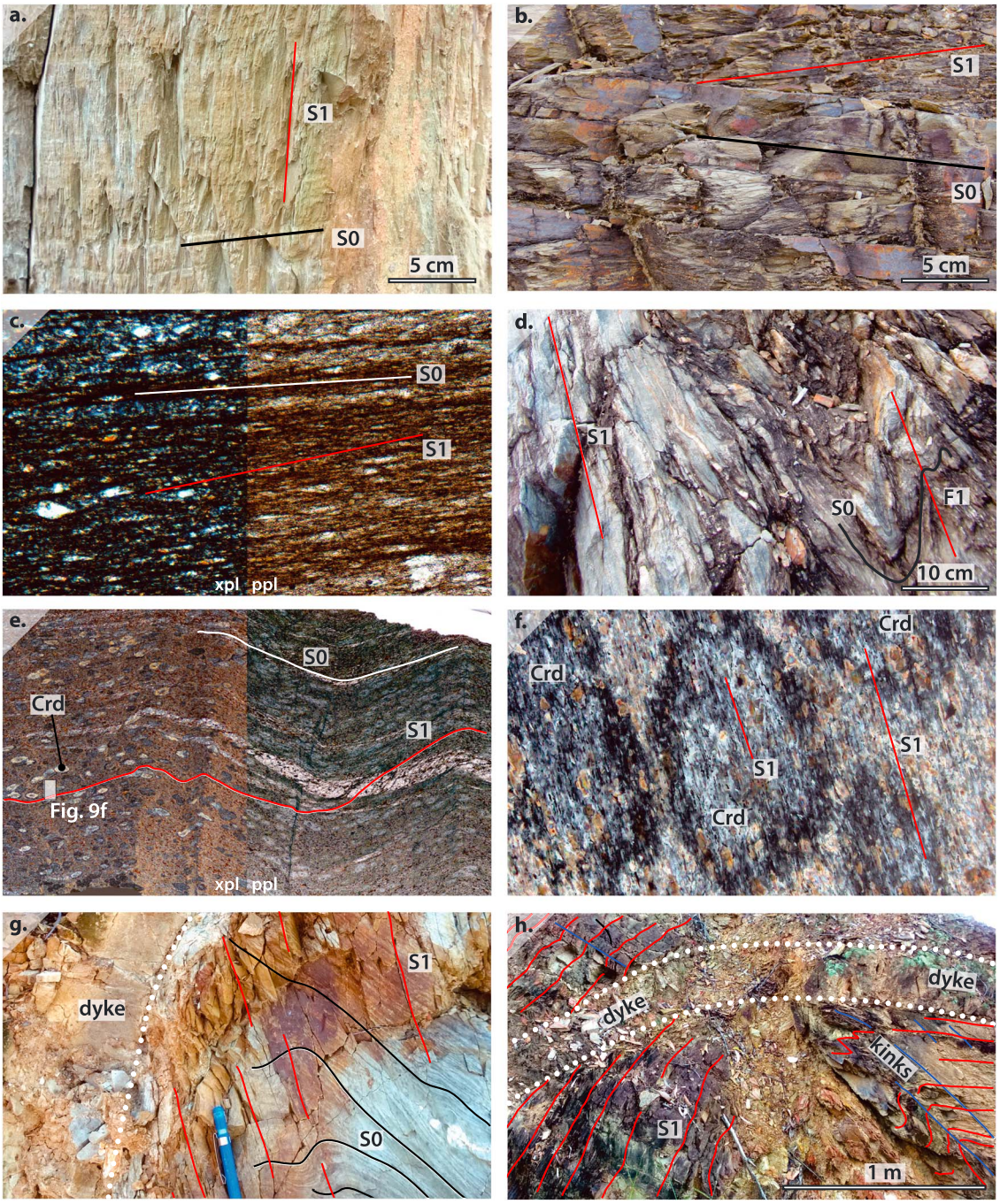

Figure 9. D_1 deformation and post-D_1 magmatism. See Figure 3 for locations and view directions. (a) Pervasive S_1 slaty cleavage and relict S_0 in slate of the Kin Kin beds; (b) S_1 in interbedded sandstone and siltstone from the Kin Kin beds; and (c) photomicrograph of slate from the Triassic Kin Kin beds. Note that S_1 is weakly developed in psammitic lithologies at microscale and mesoscale; (d) west verging parasitic F_1 fold in the Kin Kin beds; (e) cordierite poikiloblasts (now partly altered to Pinite) overprinting S_1 in hornfelsed slate. Kink bands are attributed to localized deformation during intrusion (field of view (FOV) ~ 35 mm); (f) inclusions of S_1 fabric within cordierite poikiloblasts and lack of S_1 strain shadows provide evidence for post-S_1 intrusion; (g) weathered mafic dyke cuts S_0 and S_1; and (h) weathered mafic dyke cuts S_1 in Kin Kin phyllite. Both S_1 and the dyke are folded during later kink-style deformation.

5.2. Second Deformation (D_2)

Overprinting the S_1 foliation and magmatic rocks are a series of thrust and reverse faults attributed to the second phase of deformation. D_2 structures are much weaker than D_1 structures. They occur in the Gympie Goldfield region (Figures 3 and 6e), where D_2 is correlated with a postmineralization décollement with top

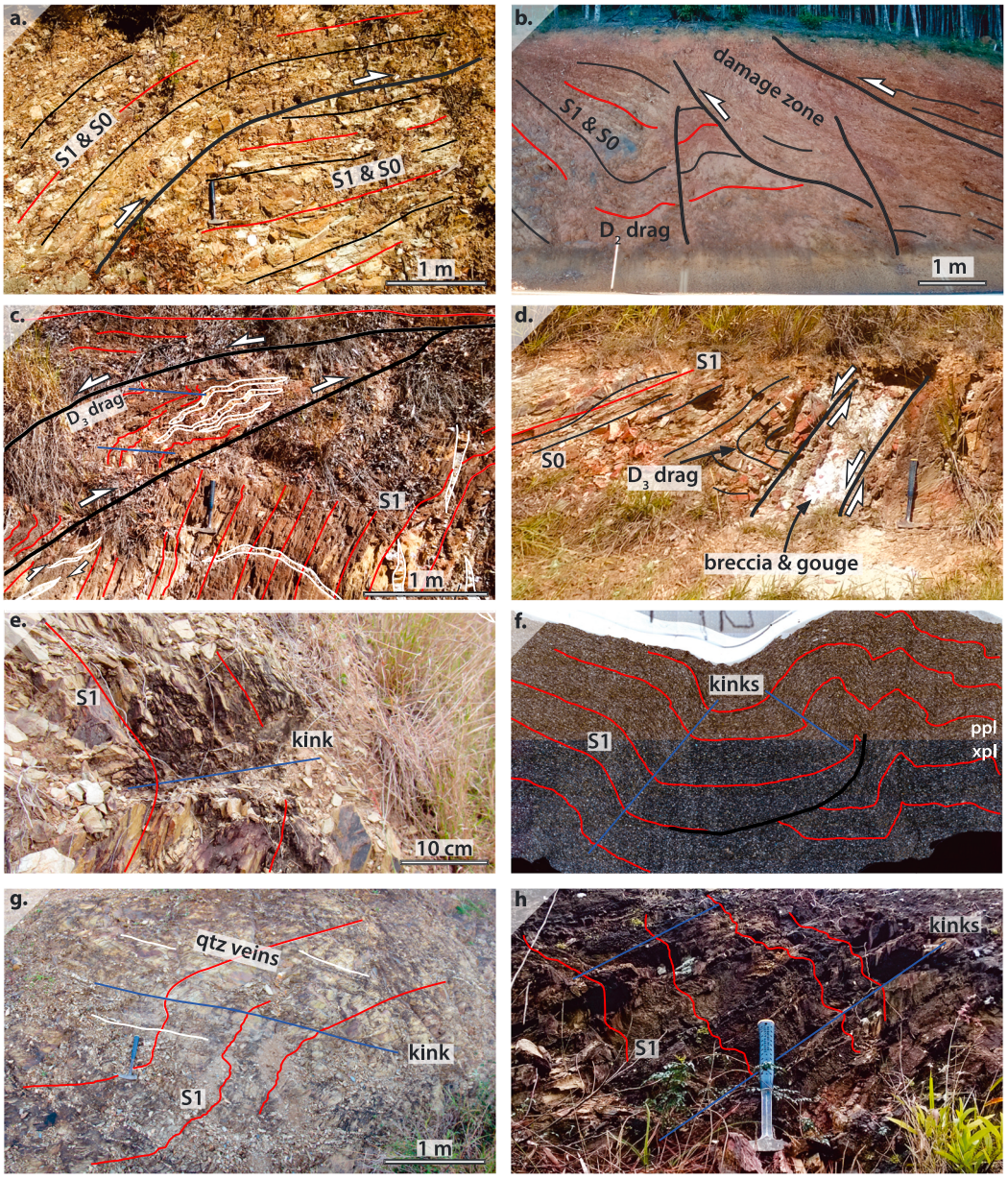

Figure 10. D_2 and D_3 deformation. See Figure 3 for locations and view directions. (a) West vergent thrust fault cuts bedding and S_1 cleavage; (b) west vergent thrust fault cuts bedding and S_1, displaying drag folding and well-developed damage zone in the footwall; (c) low-angle normal fault with folding showing normal kinematics in footwall damage zone, which truncates and locally reactivates D_2 thrust; (d) normal fault cutting cleaved bedding with well-developed fault gouge and associated drag fold; (e) shallowly inclined kink fold causes steep S_1 to dip in opposite directions; (f) microphotograph showing conjugate kink folds and fault propagation folds in Kin Kin beds slate (FOV ~35 mm); (g) moderately inclined kink fold parallel to quartz veins in shallowly dipping limb of larger conjugate kink fold; and (h) well-developed spaced kink fabric.

to the SW kinematics (Curra Break Fault) [*Crawford*, 2003]. In addition to the Curra Break Fault, other east dipping faults with reverse kinematics cut both S_0 and S_1 (Figures 6c–6e) and are correlated with D_2. D_2 structures are also developed in the eastern part of the terrane, where cleaved psammopelitic rocks are cut by several E to NE dipping thrust faults (Figure 3). Relatively minor faults exhibiting ramp-flat geometry and small duplexes are the most common structures (Figure 10a). However, some of these faults show evidence for reverse kinematics, exhibiting drag folding and brecciated zones up to several meters wide (Figure 10b), indicating that they are more significant thrusts. While the kinematics of major structures in

the area is well constrained, kinematic indicators were not observed on many minor faults, which were thus inferred from their correlation with better-constrained faults nearby (e.g., Figure 10b). Several D_2 thrusts such as the Curra Break Fault and other unnamed faults documented herein (Figures 4k, 4l, 6c, 6d, and 10c) show evidence that D_2 reverse kinematics was followed by reactivation with normal kinematics, which we attribute to D_3 extension (section 5.3).

Although D_1 and D_2 are vaguely similar in terms of orientation and kinematics, the abundance of post-S_1 dykes at an angle approaching parallelism with contractional structures such as S_1 implies a major relaxation of contractional deformation during magmatism. This is also supported by the lack of a synkinematic magmatic foliation in the Woondum Granite. These observations, coupled with the faulted eastern margin of the Woondum Granite against the Kin Kin beds (Figure 3), suggest that the granite was emplaced in the period between deformation phases D_1 and D_2. Thus, the age of the Woondum Granite provides both a minimum age constraint for D_1 and a maximum age constraint for the later thrust-related deformation D_2 (cf. section 6.1). On the basis of these observations, we consider D_1 and D_2 to be separate deformation events that were punctuated by widespread magmatism.

5.3. Third Deformation (D_3)

The third phase of deformation (D_3) involved east block down kinematics on steeply dipping normal faults and widespread kinking. Some D_2 thrusts and reverse faults appear to have a complex history as they also show evidence of normal kinematics, suggesting they have been reactivated during D_3 (Figures 4k, 4l, 6c, 6d, and 10c). The dragging of S_0 and early formed fault structures, as well as the development of D_3 cataclasite and fault gouge (Figure 6d), suggests that the dominant motion on some faults occurred during D_3 extension. Several NE dipping faults in the southern Kin Kin beds are associated with D_2 (reverse) drag folds and asymmetric strain shadows indicating reverse kinematics (Figure 4l), while the fault core contains oblique-foliated cataclasite indicating a stage of normal kinematics (Figure 4k) and suggesting they have been reactivated. In addition to reactivation of preexisting fault slip surfaces, D_3 normal faults also form shortcut faults that are subparallel to earlier thrusts (Figure 10c), or isolated normal faults displaying drag folding of S_1 and S_0 and well-developed fault gouge zones (Figure 10d).

Most normal faults observed were inferred to have relatively minor offsets based on the lithological continuity between hanging wall and footwall rocks. However, some normal faults appear to have more significant offsets as indicated by the juxtaposition of different lithologies (Figure 10d). We note, however, that the general lack of stratigraphic markers in the Gympie Terrane and particularly the Kin Kin beds makes it difficult to accurately assess the throw of most faults. At a larger scale, major extensional deformation is indicated from the stratigraphic juxtaposition of Triassic hanging wall rocks in the east of the terrane that were thrust up and against Permian rocks in the footwall to the west during D_1 and D_2. To explain this relationship, we speculate that the magnitude of D_3 extension on this fault boundary was equal to or greater than the cumulative uplift during D_1 and D_2.

Late stage development of kinks is recognized in the strongly cleaved metapelites of the Kin Kin beds, associated with widespread spaced kink bands and kink folds. F_3 kink folds and S_3 kink bands generally dip shallowly to moderately (Figure 10e), but the dip direction varies considerably due to conjugate kinks and/or younger deformation. F_3 kinks within the Kin Kin beds are heterogeneous; some areas exhibit major kink folds with interlimb angles becoming as tight as ~90°, while other areas show smaller kink bands. In many cases, kinks are associated with minor synthetic accommodation faults that either splay off or join with the S_1 cleavage (Figure 10f). In places, kinks are coincident with parallel thin quartz veins (Figure 10g). Conjugate sets of kinks are recognized in thin section (Figure 10f) and outcrop (Figure 4) and may be inferred in other areas with less contiguous outcrop by changes in kink fold vergence. A single orientation of kinks is dominant in other areas (Figure 10h).

The interpretation that many conjugate kinks formed during D_3 extension is supported by deformation experiments on foliated rocks [*Cobbold et al*., 1971; *Dewey*, 1965; *Gay and Weiss*, 1974; *Paterson and Weiss*, 1966; *Weiss*, 1980], which show that conjugate kink bands can form up to 120° apart, with the maximum compression direction bisecting the obtuse angle between the kink bands. In outcrops where the vergence and orientation of kinks clearly demonstrate that they are a conjugate set, the obtuse bisector is steeply dipping

and approximately parallel to the bulk orientation of the S_1 cleavage, thus suggesting that the kinks formed during subvertical shortening associated with extension or exhumation.

While we consider that widespread kinking occurred in association with D_3, we also recognize more than one set of kinks, including some kink folds that appeared to be associated with D_2 contraction (e.g., Figure 4j). Furthermore, the origin of several kilometer-scale angular to subangular open folds in the S_1 cleavage within the Kin Kin beds (Figure 3) remains somewhat ambiguous. One such fold occurs in the area just northeast of the Gympie goldfield, where the S_1 fabric in the Kin Kin beds makes a sharp deviation toward the east, defining a large SE plunging syncline-anticline pair (Figure 3). *Cranfield* [1999] mapped a fault-bounded sliver of the Tamaree Formation and South Curra Limestone, as well as an outlier of Maryborough Basin rocks, which appear to occupy the cores of the anticline and syncline, respectively. The involvement of Maryborough Basin rocks (Figure 2) in this deformation is also supported by the map view curvature of the regional unconformity north of the Gympie Terrane (Figure 3) despite modest topographic relief. If this unconformity has indeed been folded along with the previously described syncline-anticline pair, then deformation is of regional extent and likely occurred during or after the middle Mesozoic. While more work is needed, these folds may be related to a weakly developed pressure solution-crenulation cleavage in parts of the Kin Kin beds that was previously described by *Cranfield and Scott* [1993].

6. Discussion

6.1. Tectonic Significance of D_1 Deformation in the Gympie Terrane

Our structural analysis indicates that rocks of the Gympie Terrane were subjected to multiple phases of deformation. The earliest deformation (D_1) is significantly more pronounced than later phases and is responsible for the formation of the dominant S_1 cleavage and most of the folding in the study area. The presence of kilometer-scale overturned F_1 folds with east dipping S_1 axial planar cleavage (Figure 5) suggests that D_1 involved west vergent deformation. While lithology appears to be one control on the response to deformation, the increased intensity of D_1 in the proximity of the western edge of the Kin Kin beds suggests that the boundary between the Permian and Triassic rocks of the Gympie Terrane may be a major fault that was active during D_1. If this interpretation is correct, the strong partitioning of strain into the Kin Kin beds may be interpreted as preferential deformation in the hanging wall of a thrust sheet or décollement, while footwall rocks to the west are only deformed in the immediate vicinity of the fault itself.

The timing of D_1 must be younger than ~240 Ma, which is the maximum depositional age of the Kin Kin beds (Figure 2) [*Li et al*., 2015]. A minimum age constraint is provided by the ~232 Ma $^{40}Ar/^{39}Ar$ biotite and 223–226 Ma K/Ar ages of the crosscutting Woondum Granite ([*Webb and McDougall*, 1967], recalculated by *Cranfield* [1999], and *Easter* [2000, unpublished thesis]). Hornfelsed slate from the intrusive contact displays abundant cordierite poikiloblasts that lack S_1 strain shadows and contain abundant inclusions of fine mica parallel to S_1 (Figures 9e and 9f). These features are indicative of post-D_1 contact metamorphism, suggesting that west vergent contractional deformation (D_1) in the Gympie Terrane occurred between 240 Ma and 232 Ma. Furthermore, an increase in the intensity of post-S_1 thrusting near the eastern margin of the intrusion (Figure 3) suggests accumulation of strain against a rigid body during D_2 deformation. If the ~232 Ma age reflects crystallization rather than cooling, the Woondum Granite also provides a constraint for the maximum age of later thrust-related deformation D_2. Both the style and timing of D_1 deformation matches well with previous observations for predominantly foreland-verging deformation associated with the Hunter-Bowen Orogeny (Figure 11). We therefore consider that D_1 in the Gympie Terrane corresponds to the last phase of the Hunter-Bowen Orogeny (HBO 3) at 235–230 Ma.

The constraints on the age of D_1 deformation in the Gympie Terrane are consistent with evidence for HBO 3 deformation in the Esk Trough and Nymboida Coal Measures (Figures 1b and 11). The Esk Trough is an Early Permian to Middle Triassic basin situated in the central part of the fold belt, between the foreland basin and the Gympie Terrane (Figure 3). Deformational features in the Esk Trough are associated with a large asymmetric east vergent synclinorium, which has been attributed to backthrusting during HBO 3 [*Campbell*, 2005; *Holcombe et al*., 1997b]. This deformation must have occurred after deposition of the Middle Triassic strata but prior to the emplacement of an undeformed Upper Triassic volcanic cover sequence at ~228 Ma [*Holcombe et al*., 1997b]. The Middle Triassic Nymboida Coal Measures are possible correlatives farther south

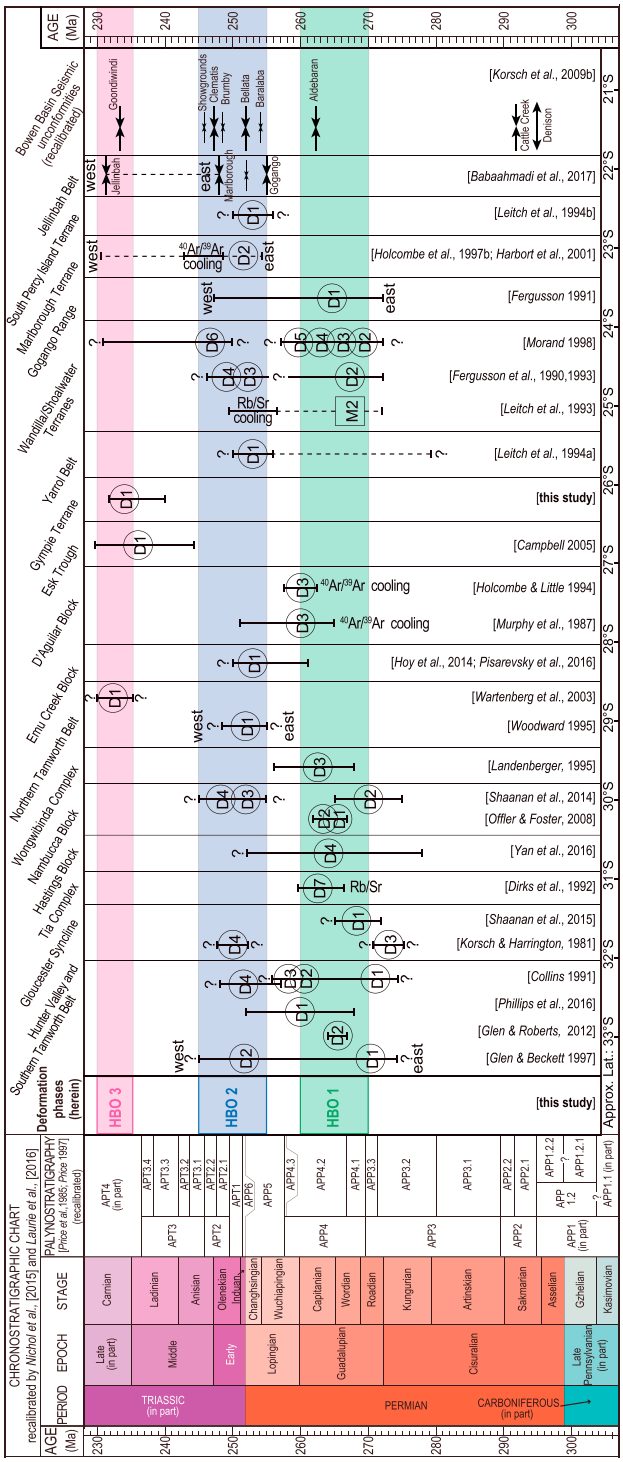

Figure 11. Time-space plot showing timing, distribution, and correlation of deformation features associated with the Hunter-Bowen Orogeny in eastern Australia [*Babaahmadi et al.*, 2017; *Campbell*, 2005; *Collins*, 1991; *Dirks et al.*, 1992; *Fergusson*, 1991; *Fergusson et al.*, 1990, 1993; *Glen and Beckett*, 1997; *Glen and Roberts*, 2012; *Harbort et al.*, 2001; *Holcombe and Little*, 1994; *Holcombe et al.*, 1997a, 1997b; *Hoy et al.*, 2014; *Korsch et al.*, 2009b; *Korsch and Harrington*, 1981; *Landenberger*, 1995; *Leitch et al.*, 1993; *Leitch et al.*, 1994a, 1994b; *Morand*, 1998; *Murphy et al.*, 1987; *Offler and Foster*, 2008; *Phillips et al.*, 2016; *Pisarevsky et al.*, 2016; *Price*, 1997; *Shaanan et al.*, 2014, 2015; *Wartenberg et al.*, 2003; *Woodward*, 1995; *Yan et al.*, 2016]. See also Figure 12.

(Figure 1c) (also recognized by *Babaahmadi et al*. [2015]) and contain a basalt unit dated by $^{40}Ar/^{39}Ar$—plagioclase at 237.0 ± 0.4 Ma [*Retallack et al*., 1993] that is unconformably overlain by extension-related basin succession dated by K/Ar at ~232 Ma [*Purdy et al*., 2013]. The maximum and minimum constraints on the age of deformation in the Nymboida Coal Measures are therefore ~237 Ma and ~232 Ma, respectively.

6.2. Time-Space Variations and Deformation Cycles of the Hunter-Bowen Orogeny

An increasing volume of data indicates that the Middle Permian to Late Triassic Hunter-Bowen Orogeny in eastern Australia was not continuous but rather involved pulses of contractional deformation and crustal thickening [*Holcombe et al*., 1997b; *Korsch et al*., 2009b; *Scheibner*, 1996; *Veevers and Morgan*, 2000] interspersed with periods of extension and transtension [*Babaahmadi et al*., 2015; *Korsch et al*., 1989]. These pulses of Hunter-Bowen deformation show significant variations in timing, duration, and deformation intensity both along and across the fold belt (Figures 11 and 12). The three broad phases of contraction discussed here (HBO1, 2, and 3) are in line with the interpretation of *Holcombe et al.* [1997b].

The first pulse of Hunter-Bowen contraction (HBO 1) began in the Middle Permian at around 265 Ma [*Holcombe et al*., 1997b], although the exact timing is not well constrained. Deformation associated with this phase is widely recognized in the northern [*Fergusson*, 1991; *Fergusson et al*., 1990, 1993], central (D'Aguilar Block) [*Holcombe and Little*, 1994; *Sliwa*, 1995] and southern [*Collins*, 1991; *Phillips et al*., 2016; *Shaanan et al*., 2014; *Woodward*, 1995] parts of the fold belt. However, during this interval, the Gympie Terrane was a site of more-or-less continuous deposition and experienced no deformation. The lack of conclusive evidence for HBO 1 deformation in the Gympie Terrane is in contrast with observations for contemporaneous deformation in the adjoining D'Aguilar Block to the west [*Holcombe and Little*, 1994; *Sliwa*, 1995], thus indicating a significant strain partitioning between inboard and outboard parts of the fold belt. Unlike the central part of the fold belt, early Hunter-Bowen deformation in the southern and northern parts involved prolonged westward propagating contraction that continued from HBO 1 to HBO 2 [*Collins*, 1991; *Fergusson*, 1991; *Fergusson et al*., 1990, 1993; *Glen and Beckett*, 1997; *Phillips et al*., 2016].

The second pulse of contractional deformation (HBO 2) likely initiated at around the Permo-Triassic boundary and was associated with a major increase in the rate of foreland basin subsidence, while sediments shed from the thickened hinterland flooded the basin and brought a change from marine to terrestrial deposition [*Brakel et al*., 2009; *Korsch and Totterdell*, 2009; *Waschbusch et al*., 2009]. Sedimentation in the Gympie Terrane mimics that in the foreland basin during HBO 2, with a transition from a marine to terrestrial depositional environment and an increase in the proportion of basement-derived (e.g., Late Devonian-Carboniferous) detrital zircons [*Li et al*., 2015]. Although the sedimentological response to HBO 2 is relatively consistent along the fold belt, pronounced along-strike changes are recognized in the timing and distribution of deformation between the northern, central, and southern parts of the fold belt (Figures 11 and 12). The most pronounced effects of HBO 2 are recognized in the north, where out-of-sequence thrusting reinitiated in the outboard part of the fold belt and involved nappe-style tectonics associated with the emplacement of the Marlborough Terrane (Figure 11) [*Harbort et al*., 2001; *Holcombe et al*., 1997b]. The advancing HBO 2 thrust front caused sequentially younger deformation toward the west [*Fergusson*, 1991; *Fergusson et al*., 1990, 1993] that deformed the synorogenic retroforeland basin sequence during HBO 3 [*Babaahmadi et al*., 2017; *Holcombe et al*., 1997b; *Korsch et al*., 2009b]. HBO 2 in the southern part of the fold belt is associated with continuing deformation on several foreland-verging thrust systems that likely initiated during HBO 1 [*Glen and Beckett*, 1997]. While it is possible that some evidence for HBO 2 deformation in the foreland basin may be concealed by Mesozoic cover, available observations suggest that HBO 2 was weaker or entirely absent in the central part of the fold belt, in comparison to the northern and southern parts (Figures 11 and 12).

The final phase of Hunter-Bowen deformation (HBO 3) at approximately 235–230 Ma is recorded in the Gympie Terrane and Esk Trough (in the outboard central part of the fold belt) and is also well developed in the northern parts of the retroforeland basin (Figure 12). Middle Triassic rocks in the foreland basin were involved in widespread folding and uplift during HBO 3 in the Middle to Late Triassic [*Babaahmadi et al*., 2017; *Campbell et al*., 2017; *Korsch et al*., 2009b]. This deformation resulted in regional folding, west directed thrusting, reactivation of normal faults, basin inversion, and up to ~4 km of erosion prior to the deposition of latest Triassic rocks above a significant angular unconformity [*Korsch et al*., 2009b]. Middle Triassic strata in the central and southerly parts of the foreland basin were also involved in this

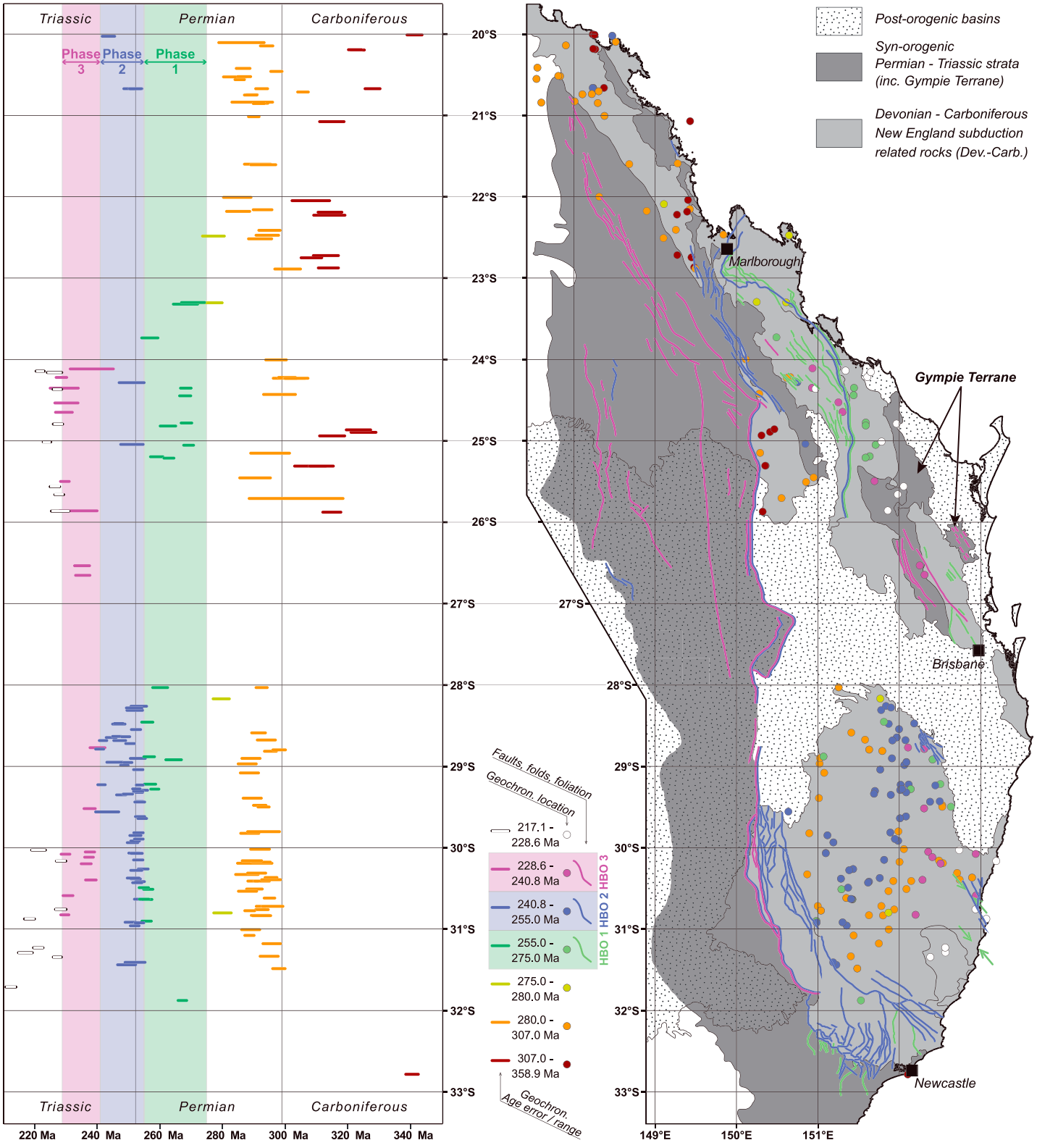

Figure 12. Pulses of deformation and magmatism (HBO 1–3 are color coded) related to Late Paleozoic to Early Mesozoic orogenesis in eastern Australia. The age versus latitude diagram (left) shows age ranges or age errors for magmatism on the horizontal axis. The latitude on the vertical axis also corresponds to the grid on the map of eastern Australia to the right, which highlights the location of geochronological data points representing magmatism (circles) and Hunter-Bowen deformation (thick lines). The compiled age data presented herein are provided in supporting information S1. See Figure 11 for references and correlation of deformation.

deformation [*Totterdell et al*., 2009]. However, when compared to the northern part, deformation was more restricted to the region surrounding the eastern boundary faults (Figure 12), *Babaahmadi et al*., 2017]. In the central part (Gympie Terrane and Esk Trough), major HBO 3 deformation occurred outboard from much of the contemporaneous fold-thrust belt in the retroforeland basin, rather than by continued foreland propagation of the thrust front, indicating strain partitioning between the inboard (foreland basin) and outboard parts of the fold-thrust belt. It appears that overall, HBO 3 deformation was stronger and more widespread in the northern and central fold belt in comparison to the southern part (Figures 11 and 12), suggesting further strain partitioning along strike of the fold belt.

6.3. Geodynamic Implications on the Episodic Behavior of Accretionary Orogens

Previous authors have suggested that the Gympie Terrane was an exotic intraoceanic island arc that collided with the continent at either ~253 Ma or ~235 Ma (corresponding to our HBO 2 and HBO 3, respectively) and triggered Hunter-Bowen contractional tectonism [*Buckman et al*., 2015; *Harrington and Korsch*, 1985; *Nutman et al*., 2013; *Scheibner*, 1996]. However, arc-continent collision during HBO 2 or HBO 3 cannot explain the earlier onset of orogeny (i.e., HBO 1), especially given that the Gympie Terrane was not exotic or isolated from the continent [*Sivell and McCulloch*, 2001; *Li et al*., 2015]. Our field observations from the contact between the Gympie Terrane and D'Aguilar Block do not support the idea that this contact is a major lithospheric-scale suture zone, but rather, these faults only show evidence for moderate strike-slip displacement (Figure 8). While our mapping of the terrane boundary could not completely rule out a paraautochthonous origin of the Gympie Terrane, the contribution of Australian continental crust to the magmas and sedimentary rocks of the Gympie Terrane [*Sivell and McCulloch*, 2001; *Li et al*., 2015; *Korsch et al*., 2009c] suggests autochthoneity with respect to the adjoining rocks [*Li et al*., 2015] and hence that orogenesis could not have been primarily driven by arc-continent collision. Alternatively, it is possible that the Gympie Terrane magmatic arc was built on an outboard migrating continental ribbon following rifting in the Early Permian [*Collins and Richards*, 2008], although this remains to be tested by means of paleomagnetic and structural investigations. Even if we assume that a paraautochthonous Gympie Terrane (±continental ribbon substrate) was reaccreted to the continent following the closure of a marginal sea that separated the crustal mass from the Australian Continent [*Collins and Richards*, 2008], docking must have been preceded by a pull-push switch in the mode of tectonism [e.g., *Lister and Forster*, 2009]. In other words, a tectonic mode switch occurred from Early Permian extension and slab retreat [*Holcombe et al*., 1997a; *Korsch et al*., 2009a] to slab advance [*Holcombe et al*., 1997b]. In this model, the accretion of a crustal mass may have contributed to a localized and transient increase in plate coupling at the time of accretion, but docking occurred as a consequence of the switch to slab advance, implying that Hunter-Bowen Orogeny was triggered by another geodynamic mechanism.

The suggestion that Hunter-Bowen Orogeny was not necessarily driven by accretion of an individual terrane or the subduction of anomalously buoyant crust appears reasonable when one considers the scale of contemporaneous deformation (i.e., the Gondwanide Orogeny, Figure 13) along the length of the paleo-Pacific margin of Gondwana [*Cawood*, 2005; *Cawood et al*., 2011; *Trouw and De Wit*, 1999; *Veevers*, 1989]. Such episodes of Permian-Triassic deformation are recognized in the Ellsworth Mountains (Antarctica), Cape Fold Belt (South Africa), Falkland Islands, and La Sierra de la Ventana (Argentina) [*Curtis*, 1997, 2001; *Hansma et al*., 2015; *Johnston*, 2000; *López-Gamundí*, 2006; *Mukasa and Dalziel*, 2000; *Vaughan and Pankhurst*, 2008]. The length of the Gondwanide Orogen is too extensive to be caused solely by factors that influence coupling at the subcontinental scale. It is more likely that pulses of deformation recognized locally throughout the south Gondwanan margin were parts of a larger orogenic cycle [e.g., *Lister et al*., 2001] that were perhaps ultimately controlled by a global tectonic plate reorganization. For example, *Cawood and Buchan* [2007] proposed that the change in plate configuration during the final assembly of Pangea led to a change in the number of plates and their kinematics, potentially allowing greater convergence rates and coupling at the exterior subduction boundaries. However, much of the Pangean margin experienced widespread extension immediately following terminal Variscan deformation at approximately 320–300 Ma [*Veevers*, 2013]. The resumption of arc magmatism and increased coupling along the south Gondwanan margin appeared to have initiated in the western sector in the Early Permian, propagating toward the east until the entire margin was affected from the Middle Permian onward [*Veevers*, 2004]. In contrast, the north Gondwanan margin experienced continued extension from the Late to Early Permian onward with the opening of the Meso-Tethyan Ocean and northward translation of the South Qiangtang, Sibumasu, and Lhasa terranes (i.e., the

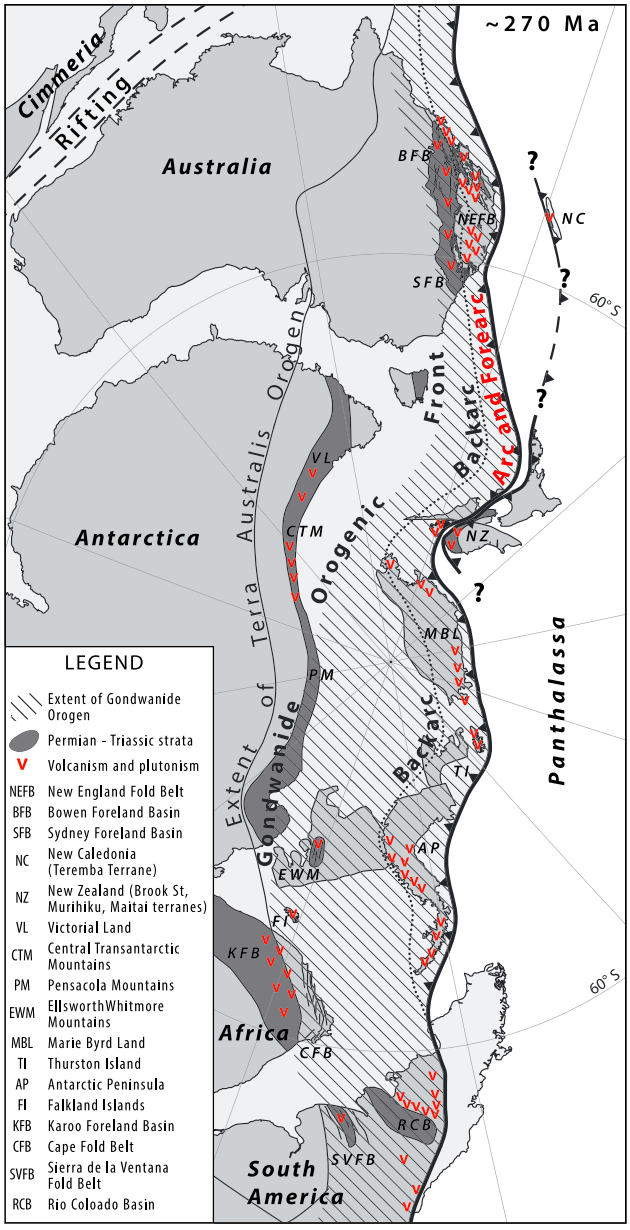

Figure 13. Reconstruction of Gondwana at ~270 Ma (GPLATES orthographic projection centered on 85°S 142°E) [after *Domeier and Torsvik*, 2014] showing the distribution of deformation and magmatism related to the Gondwanide Orogeny. Permian-Triassic Hunter-Bowen deformation and magmatism in east Australia is from this work and references herein. Volcaniclastic deposits in the central Transantarctic Mountains at ~260–240 Ma from *Elliot et al.* [2016]. Marie Byrd Land geology based on *Mukasa and Dalziel* [2000]. Tectonic setting of the Antarctic Peninsula after *Burton-Johnson and Riley* [2015] with Permian-Triassic metamorphism and magmatism after *Millar et al.* [2002], *Riley et al.* [2012], and *Castillo et al.* [2016]. The position of New Zealand's south island and the Brook Street Terrane during arc accretion are from *Davey* [2005] with revised timing according to *McCoy-West et al.* [2014]. South African Cape Fold Belt deformation at ~276–246 Ma is from *Hansma et al.* [2015] and explosive volcanism at ~274–250 Ma is from *McKay et al.* [2015] and references therein. Carboniferous-Permian collision of Patagonia with South America after *Pankhurst et al.* [2006]. Permian volcanism in South America and Africa is after *López-Gamundí* [2006].

Cimmerian continent) [*Metcalfe*, 2013] temporally linked with the widespread Gondwanide deformation at ~275–270 Ma. Although the geodynamics of post-Pangean plate reorganization appears to be quite complex, changes to the number of tectonic plates and their motion provide a feasible explanation as to how enhanced coupling could simultaneously affect much of the paleo-Pacific margin of Gondwana without requiring the subduction of anomalously buoyant crust or terrane accretion to occur simultaneously over thousands of kilometers along the margin. Although we suggest that widespread orogenesis was triggered by these large-scale plate kinematic changes, processes that operate at shorter length and timescales, such as ribbon or microcontinent accretion, as well as variations in the buoyancy, thickness, and bathymetric relief of the subducted lithosphere, may all contribute to variations in the timing, intensity, and partitioning of specific deformation phases within the larger orogenic cycle.

The suggestion that plate coupling during orogenesis is affected by the superposition of different mechanisms acting at a range of scales has been documented in modern orogenic belts. For example, intense orogenesis throughout the Andes from around 30 Ma was thought to result from coupled plate kinematic changes associated with an abrupt deceleration in the northeastward motion of the African Plate and the consequent acceleration of the westward moving South American Plate [*Silver et al.*, 1998; *Sobolev and Babeyko*, 2005]. At the regional scale, spatiotemporal variations in the intensity of deformation result from terrane accretion or from more subtle changes in the subduction dynamics associated, for

example, with variations in slab buoyancy or lithospheric thickness [e.g., *Capitanio et al*., 2011; *Horton and Fuentes*, 2016; *Martinod et al*., 2013; *Rosenbaum and Mo*, 2011]. While it appears that large-scale plate kinematics were the primary control on widespread Andean orogenesis in the Cenozoic, the superposition of both continental and regional scale mechanisms resulted in major along-strike differences, which are evident in the difference between the spectacular central Andes and the more subdued southern Andes. The recognition that widespread Andean orogenesis was triggered by a kinematic change in African Plate motion, and that local variations in subduction dynamics can influence heterogeneity within the orogen, provides an intriguing modern analogue for the fundamental processes that affected orogenic cycles in ancient orogens.

7. Conclusions

The Hunter-Bowen Orogeny involved several phases of deformation spanning the Middle Permian to the Middle to Late Triassic. Permian to Middle Triassic rocks of the Gympie Terrane were affected by overturned folding and related cleavage development that likely occurred during the third and final phase of the Hunter-Bowen Orogeny at approximately 235–230 Ma. This terminal Hunter-Bowen deformation was widespread in eastern Australia and was responsible for uplift and development of a regional angular unconformity in both the foreland and hinterland regions. Similarly to many other parts of eastern Australia, Hunter-Bowen deformation in the Gympie Terrane was related to a foreland-verging fold-and-thrust system, albeit one that occurred outboard from much of the contemporaneous fold-and-thrust belt. The Middle-Late Triassic deformation was strongest in the northern and central part of the fold belt, suggesting that Hunter-Bowen deformation was associated with along-strike variations in the amount of coupling across the subduction zone. Although local perturbations occur in the timing and intensity of individual short-lived phases of deformation, deformation features that mark the Gondwanide Orogeny may be correlated throughout eastern Australia and more widely along the Gondwanan margin. Our results do not support previous suggestions that the Hunter-Bowen Orogeny was caused by the accretion of the Gympie Terrane, and we see no need to invoke a unique mechanism for orogenesis at this part of the orogenic belt. Rather, the Hunter-Bowen deformation was inevitably linked to the other sectors of the Gondwanide Orogen, which was possibly initiated by changes in global plate configuration and increased convergence rates.

Acknowledgments

This paper is dedicated to the commemoration of our friend and colleague Marco Beltrando. The authors would like to thank Rod Holcombe, Uri Shaanan, and Alex Slade for their insightful comments, discussions, and assistance in the field. Suggestions from two anonymous reviewers on an earlier version greatly improved the focus and direction of the paper. Reviewers Richard Glen and William Collins are also thanked for their perspectives and helpful criticisms, which further improved the manuscript. We also thank the participants of the SGTSG 2015 postconference field trip to the Gympie Terrane, who helped us appreciate our observations in light of the structural and tectonic evolution of eastern Australia. Finally, we acknowledge the ideas and contribution of the many authors that have contributed to the proceedings of various New England Orogen conferences since 1982. This work was funded by the Australian Research Council grant DP130100130, and Derek Hoy acknowledges the support of an Australian Government Research Training Program Scholarship. The authors disclose that they are not aware of any financial or scientific conflicts of interest with respect to this paper. The supporting geochronological data are available in the supporting information "S1" and further information can be obtained by contacting the authors.

References

Aitchison, J. C., and S. Buckman (2012), Accordion vs. Quantum tectonics: Insights into continental growth processes from the Paleozoic of eastern Gondwana, *Gondwana Res.*, *22*(2), 674–680.

Arnold, G. (1996), Geology of the southern Gympie Goldfield from core logging and implications for mineralisation, *Annual Report Rep. QDEX Report #28999*, G.O. Arnold Ore Search Consulting.

Babaahmadi, A., and G. Rosenbaum (2014a), Late Cenozoic intraplate faulting in eastern Australia, *J. Struct. Geol.*, *69*(Part A), 59–74.

Babaahmadi, A., and G. Rosenbaum (2014b), Late Mesozoic and Cenozoic wrench tectonics in eastern Australia: Insights from the North Pine Fault System (southeast Queensland), *J. Geodyn.*, *73*, 83–99.

Babaahmadi, A., G. Rosenbaum, and J. Esterle (2015), Alternating episodes of extension and contraction during the Triassic: Evidence from Mesozoic sedimentary basins in eastern Australia, *Aust. J. Earth Sci.*, 1–17.

Babaahmadi, A., R. Sliwa, J. Esterle, and G. Rosenbaum (2017), The development of a Triassic fold-thrust belt in a synclinal depositional system, Bowen Basin (eastern Australia), *Tectonics*, *36*, 51–77, doi:10.1002/2016TC004297.

Beltrando, M., J. Hermann, G. S. Lister, and R. Compagnoni (2007), On the evolution of orogens: Pressure cycles and deformation mode switches, *Earth Planet. Sci. Lett.*, *256*(3–4), 372–388.

Brakel, A. T., J. M. Totterdell, A. T. Wells, and M. G. Nicoll (2009), Sequence stratigraphy and fill history of the Bowen Basin, Queensland, *Aust. J. Earth Sci.*, *56*(3), 401–432.

Buckman, S., A. P. Nutman, J. C. Aitchison, J. Parker, S. Bembrick, T. Line, H. Hidaka, and T. Kamiichi (2015), The Watonga Formation and Tacking Point Gabbro, Port Macquarie, Australia: Insights into crustal growth mechanisms on the eastern margin of Gondwana, *Gondwana Res.*, *28*(1), 133–151.

Burton-Johnson, A., and T. R. Riley (2015), Autochthonous v. Accreted terrane development of continental margins: A revised in situ tectonic history of the Antarctic peninsula, *J. Geol. Soc.*, *172*(6), 822–835.

Campbell, L. M. (2005), Basin analysis and tectonic evolution of the Esk Trough in southeast Queensland, *Document # THE18382*, 237 pp., PhD thesis, The Univ. of Queensland, Brisbane, QLD.

Campbell, M. J., U. Shaanan, and C. Verdel (2017), Fold interference patterns in the Bowen Basin, northeastern Australia, *Aust. J. Earth Sci.*, doi:10.1080/08120099.2017.1334704.

Capitanio, F. A., C. Faccenna, S. Zlotnik, and D. R. Stegman (2011), Subduction dynamics and the origin of Andean orogeny and the Bolivian orocline, *Nature*, *480*(7375), 83–86.

Castillo, P., C. M. Fanning, F. Hervé, and J. P. Lacassie (2016), Characterisation and tracing of Permian magmatism in the south-western segment of the Gondwanan margin; U–Pb age, Lu–Hf and O isotopic compositions of detrital zircons from metasedimentary complexes of northern Antarctic Peninsula and western Patagonia, *Gondwana Res.*, *36*, 1–13.

Cawood, P. A. (1984), The development of the SW Pacific Margin of Gondwana: Correlations between the Rangitata and New-England Orogens, *Tectonics*, *3*(5), 539–553, doi:10.1029/TC003i005p00539.

Cawood, P. A. (2005), Terra Australis Orogen: Rodinia breakup and development of the Pacific and Iapetus margins of Gondwana during the Neoproterozoic and Paleozoic, *Earth Sci. Rev.*, *69*(3–4), 249–279.
Cawood, P. A., and C. Buchan (2007), Linking accretionary orogenesis with supercontinent assembly, *Earth Sci. Rev.*, *82*(3–4), 217–256.
Cawood, P. A., E. C. Leitch, R. E. Merle, and A. A. Nemchin (2011), Orogenesis without collision: Stabilizing the Terra Australis accretionary orogen, eastern Australia, *Geol. Soc. Am. Bull.*, *123*(11–12), 2240–2255.
Cloos, M. (1993), Lithospheric buoyancy and collisional orogenesis: Subduction of oceanic plateaus, continental margins, island arcs, spreading ridges, and seamounts, *Geol. Soc. Am. Bull.*, *105*(6), 715–737.
Cobbold, P. R., J. W. Cosgrove, and J. M. Summers (1971), Development of internal structures in deformed anisotropic rocks, *Tectonophysics*, *12*(1), 23–53.
Collins, W. J. (1991), A reassessment of the Hunter-Bowen Orogeny: Tectonic implications for the southern New-England Fold Belt, *Aust. J. Earth Sci.*, *38*(4), 409–423.
Collins, W. J. (2002), Hot orogens, tectonic switching, and creation of continental crust, *Geology*, *30*(6), 535–538.
Collins, W. J., and S. W. Richards (2008), Geodynamic significance of S-type granites in circum-Pacific orogens, *Geology*, *36*(7), 559–562.
Collot, J., M. Vendé-Leclerc, P. Rouillard, Y. Lafoy, and L. Géli (2012), Map helps unravel complexities of the southwestern Pacific Ocean, *Eos Trans. AGU*, *93*(1), 1–2.
Cranfield, L. (1999), Gympie Special Sheet 9445, Part 9545, Queensland 1: 100 000 Geological Map Commentary Rep., Queensland Dep. of Mines and Energy, Brisbane.
Cranfield, L., and M. Scott (1993), Geology of the Gympie 1: 100 000 Special area (9445, 9545), Queensland Dep. of Mines and Energy, Brisbane.
Crawford, M. A. (2003), The geometry and deformational history of the Curra "Break" Fault, Gympie Goldfields, 101 pp, The Univ. of Queensland, St. Lucia, Queensland.
Curtis, M. L. (1997), Gondwanian age dextral transpression and spatial kinematic partitioning within the heritage range, Ellsworth Mountains, West Antarctica, *Tectonics*, *16*(1), 172–181, doi:10.1029/96TC01418.
Curtis, M. L. (2001), Tectonic history of the Ellsworth Mountains, West Antarctica: Reconciling a Gondwana enigma, *Bull. Geol. Soc. Am.*, *113*(7), 939–958.
Davey, F. J. (2005), A Mesozoic crustal suture on the Gondwana margin in the New Zealand region, *Tectonics*, *24*, TC4006, doi:10.1029/2004TC001719.
Day, R. W., C. G. Murray, and W. G. Whitaker (1978), The eastern part of the Tasman Orogenic Zone, *Tectonophysics*, *48*(3–4), 327–364.
Dewey, J. F. (1965), Nature and origin of kink-bands, *Tectonophysics*, *1*(6), 459–494.
Dirks, P. H. G. M., G. Lennox, and S. E. Shaw (1992), Tectonic implications of two Rb/Sr biotite dates for the Tia granodiorite, southern New England Fold Belt, NSW, Australia, *Aust. J. Earth Sci.*, *39*(1), 111–114.
Domeier, M., and T. H. Torsvik (2014), Plate tectonics in the late Paleozoic, *Geosci. Front.*, *5*(3), 303–350.
Du Toit, A. L. (1937), *Our Wandering Continents: An Hypothesis of Continental Drifting*, Oliver and Boyd, Edinburgh.
Easter, S. E. (2000), The spatial and temporal relationship between mineralisation and magmatism in mesothermal gold deposits: An example from the Gympie Goldfield, southeast Queensland, 85 pp., Univ. of Queensland.
Elliot, D. H., C. M. Fanning, J. L. Isbell, and S. R. Hulett (2016), The Permo-Triassic Gondwana sequence, central Transantarctic Mountains, Antarctica: Zircon geochronology, provenance, and basin evolution, *Geosphere*, GES01345. 01341.
Fergusson, C. L. (1991), Thin-skinned thrusting in the northern New England Orogen, central Queensland, Australia, *Tectonics*, *10*(4), 797–806, doi:10.1029/90TC02708.
Fergusson, C. L., R. A. Henderson, and E. C. Leitch (1990), Structural history and tectonics of the Palaeozoic Shoalwater and Wandilla terranes, northern New England Orogen, Queensland, *Aust. J. Earth Sci.*, *37*(4), 387–400.
Fergusson, C. L., R. A. Henderson, E. C. Leitch, and H. Ishiga (1993), Lithology and structure of the Wandilla terrane, Gladstone-Yeppoon district, central Queensland, and an overview of the Palaeozoic subduction complex of the New England Fold Belt, *Aust. J. Earth Sci.*, *40*(4), 403–414.
Gay, N. C., and L. E. Weiss (1974), The relationship between principal stress directions and the geometry of kinks in foliated rocks, *Tectonophysics*, *21*(3), 287–300.
Glen, R. A. (2013), Refining accretionary orogen models for the Tasmanides of eastern Australia, *Aust. J. Earth Sci.*, *60*(3), 315–370.
Glen, R. A., and J. Beckett (1997), Structure and tectonics along the inner edge of a foreland basin: The Hunter Coalfield in the northern Sydney Basin, New South Wales, *Aust. J. Earth Sci.*, *44*(6), 853–877.
Glen, R. A., and J. Roberts (2012), Formation of oroclines in the New England Orogen, eastern Australia, *J. Virtual Explor.*, *43*(3).
Hansma, J., E. Tohver, C. Schrank, F. Jourdan, and D. Adams (2015), The timing of the Cape Orogeny: New $^{40}Ar/^{39}Ar$ age constraints on deformation and cooling of the Cape Fold Belt, South Africa, *Gondwana Res.*, *32*, 122–137.
Harbort, T. A., R. J. Holcombe, P. M. Vasconcelos, and C. R. Fielding (2001), Latest Permian emplacement of the Marlborough Block duplex: The major mountain-building phase of the Hunter-Bowen Orogeny in the northern NEFB, paper presented at Geological Society of Australia Abstracts, Geological Society of Australia; 1999.
Harrington, H. (1974), The Tasman geosyncline in Australia, in *The Tasman Geosyncline—A Symposium*, edited by A. K. Denmead, G. W. Tweedale and A. F. Wilson, pp. 383–407, Geol. Soc. of Australia, (Qld Div.), Brisbane, Queensland.
Harrington, H., and R. Korsch (1985), Late Permian to Cainozoic tectonics of the New England Orogen, *Aust. J. Earth Sci.*, *32*(2), 181–203.
Holcombe, R. J., and T. A. Little (1994), Blueschists of the New England Orogen: Structural development of the Rocksberg Greenstone and associated units near Mt Mee, southeastern Queensland, *Aust. J. Earth Sci.*, *41*(2), 115–130.
Holcombe, R. J., C. J. Stephens, C. R. Fielding, D. Gust, T. A. Little, R. Sliwa, J. Kassan, J. McPhie, and A. Ewart (1997a), Tectonic evolution of the northern New England Fold Belt: The Permian–Triassic Hunter–Bowen event, paper presented at Tectonics and metallogenesis of the New England Orogen, Special Publication of the Geological Society of Australia.
Holcombe, R. J., C. J. Stephens, C. R. Fielding, D. Gust, T. A. Little, R. Sliwa, J. McPhie, and A. Ewart (1997b), Tectonic evolution of the northern New England Fold Belt: Carboniferous to Early Permian transition from active accretion to extension, paper presented at Tectonics and metallogenesis of the New England Orogen, Special Publication of the Geological Society of Australia.
Horton, B. K., and F. Fuentes (2016), Sedimentary record of plate coupling and decoupling during growth of the Andes, *Geology*, *44*(8), 647–650.
Hoy, D., G. Rosenbaum, R. Wormald, and U. Shaanan (2014), Geology and geochronology of the Emu Creek Block (northern New South Wales, Australia) and implications for oroclinal bending in the New England Orogen, *Aust. J. Earth Sci.*, *61*(8), 1109–1124.
Huang, C.-Y., P. B. Yuan, C.-W. Lin, T. K. Wang, and C.-P. Chang (2000), Geodynamic processes of Taiwan arc–continent collision and comparison with analogs in Timor, Papua New Guinea, Urals and Corsica, *Tectonophysics*, *325*(1–2), 1–21.

Jenkins, R. B., B. Landenberger, and W. J. Collins (2002), Late Palaeozoic retreating and advancing subduction boundary in the New England Fold Belt, New South Wales, *Aust. J. Earth Sci.*, *49*(3), 467–489.
Johnston, S. T. (2000), The Cape Fold Belt and Syntaxis and the rotated Falkland Islands: Dextral transpressional tectonics along the southwest margin of Gondwana, *J. Afr. Earth Sci.*, *31*(1), 51–63.
Korsch, R. J., and J. M. Totterdell (2009), Subsidence history and basin phases of the Bowen, Gunnedah and Surat Basins, eastern Australia, *Aust. J. Earth Sci.*, *56*(3), 335–353.
Korsch, R. J., and H. J. Harrington (1981), Stratigraphic and structural synthesis of the New England Orogen, *J. Geol. Soc. Aust.*, *28*(1–2), 205–226.
Korsch, R. J., P. E. O'Brien, M. J. Sexton, K. D. Wake-Dyster, and A. T. Wells (1989), Development of Mesozoic transtensional basins in easternmost Australia, *Aust. J. Earth Sci.*, *36*(1), 13–28.
Korsch, R. J., J. M. Totterdell, D. L. Cathro, and M. G. Nicoll (2009a), Early Permian east Australian Rift System, *Aust. J. Earth Sci.*, *56*(3), 381–400.
Korsch, R. J., J. M. Totterdell, T. Fomin, and M. G. Nicoll (2009b), Contractional structures and deformational events in the Bowen, Gunnedah and Surat Basins, eastern Australia, *Aust. J. Earth Sci.*, *56*(3), 477–499.
Korsch, R. J., C. J. Adams, P. Black, D. A. Foster, G. Fraser, C. G. Murray, C. Foudoulis, and W. L. Griffin (2009c), Geochronology and provenance of the Late Paleozoic accretionary wedge and Gympie Terrane, New England Orogen, eastern Australia, *Aust. J. Earth Sci.*, *56*(5), 655–685.
Lallemand, S. E., J. Malavieille, and S. Calassou (1992), Effects of oceanic ridge subduction on accretionary wedges: Experimental modeling and marine observations, *Tectonics*, *11*(6), 1301–1313, doi:10.1029/92TC00637.
Landenberger, B. (1995), Tectonic implications of Rb_Sr biotite ages for the Hillgrove Plutonic Suite, New England Fold Belt, N.S.W., Australia, *Precambrian Res.*, *71*(1–4), 251–263.
Laurie, J. R., et al. (2016), Calibrating the middle and late Permian palynostratigraphy of Australia to the geologic time-scale via U–Pb zircon CA-IDTIMS dating, *Aust. J. Earth Sci.*, *63*(6), 701–730.
Leitch, E. C., C. L. Fergusson, R. A. Henderson, and V. J. Morand (1994a), Ophiolitic and metamorphic rocks in the Percy Isles and Shoalwater Bay region, New England fold belt, central Queensland, *Aust. J. Earth Sci.*, *41*(6), 571–579.
Leitch, E. C., C. L. Fergusson, R. A. Henderson, and V. J. Morand (1994b), Late Palaeozoic arc flank and fore-arc basin sequence of the New England fold belt in the stanage bay region, central Queensland, *Aust. J. Earth Sci.*, *41*(4), 301–310.
Leitch, E. C., V. J. Morand, C. L. Fergusson, R. A. Henderson, and P. F. Carr (1993), Accretion and post-accretion metamorphism in subduction complex terranes of the New England fold belt, eastern Australia, *J. Metamorph. Geol.*, *11*(3), 309–318.
Li, P. F., G. Rosenbaum, and D. Rubatto (2012), Triassic asymmetric subduction rollback in the southern New England Orogen (eastern Australia): The end of the Hunter-Bowen Orogeny, *Aust. J. Earth Sci.*, *59*(6), 965–981.
Li, P. F., G. Rosenbaum, J. Yang, and D. Hoy (2015), Australian-derived detrital zircons in the Permian-Triassic Gympie terrane (eastern Australia): Evidence for an autochthonous origin, *Tectonics*, *34*, 858–874, doi:10.1002/2015TC003829.
Lister, G. S., and M. A. Forster (2009), Tectonic mode switches and the nature of orogenesis, *Lithos*, *113*(1–2), 274–291.
Lister, G. S., M. A. Forster, and T. J. Rawling (2001), Episodicity during orogenesis, *Geol. Soc. London, Spec. Publ.*, *184*(1), 89–113.
López-Gamundí, O. (2006), Permian plate margin volcanism and tuffs in adjacent basins of west Gondwana: Age constraints and common characteristics, *J. S. Am. Earth Sci.*, *22*(3–4), 227–238.
Martinod, J., B. Guillaume, N. Espurt, C. Faccenna, F. Funiciello, and V. Regard (2013), Effect of aseismic ridge subduction on slab geometry and overriding plate deformation: Insights from analogue modeling, *Tectonophysics*, *588*, 39–55.
Matthai, S., M. Etheridge, and D. Henley (1991), Structural analysis and interpretation of gold mineralisation in the Gympie goldfield, QDEX Report #24483, 56 pp, Etheridge & Henley Geoscience Consultants, Gympie, Queensland.
McCoy-West, A., N. Mortimer, and T. Ireland (2014), U–Pb geochronology of Permian plutonic rocks, Longwood Range, New Zealand: Implications for Median Batholith–Brook Street Terrane relations, *N. Z. J. Geol. Geophys.*, *57*(1), 65–85.
McKay, M. P., A. Weislogel, A. Fildani, R. L. Brunt, D. M. Hodgson, and S. S. Flint (2015), U-PB zircon tuff geochronology from the Karoo Basin, South Africa: Implications of zircon recycling on stratigraphic age controls, *Int. Geol. Rev.*, *57*(4), 393–410.
Metcalfe, I. (2013), Gondwana dispersion and Asian accretion: Tectonic and palaeogeographic evolution of eastern Tethys, *J. Asian Earth Sci.*, *66*, 1–33.
Millar, I. L., J. Pankhurst, and C. M. Fanning (2002), Basement chronology of the Antarctic Peninsula: Recurrent magmatism and anatexis in the Palaeozoic Gondwana Margin, *J. Geol. Soc.*, *159*(2), 145–157.
Morand, V. J. (1998), Structure of the Broome Head Metamorphics and related rocks in the Shoalwater Bay area, northern New England Fold Belt, *Aust. J. Earth Sci.*, *45*(1), 155–167.
Mukasa, S. B., and I. W. Dalziel (2000), Marie Byrd Land, West Antarctica: Evolution of Gondwana's Pacific margin constrained by zircon U-Pb geochronology and feldspar common-Pb isotopic compositions, *Geol. Soc. Am. Bull.*, *112*(4), 611–627.
Murphy, P., H. Schwarzbock, L. C. Cranfield, I. W. Withnall, and C. G. Murray (1976), Geology of the Gympie 1: 250 000 sheet area, Geol. Surv. of Queensland.
Murphy, P., D. Trezise, L. Hutton, and L. Cranfield (1987), 1: 100000 Geological Map commentary, Caboolture sheet 9443 Queensland, Geol. Surv. of Queensland, Brisbane.
Murray, C. G., C. L. Fergusson, P. G. Flood, W. G. Whitaker, and R. J. Korsch (1987), Plate tectonic model for the carboniferous evolution of the New-England Fold Belt, *Aust. J. Earth Sci.*, *34*(2), 213–236.
Nicoll, R. S., J. L. McKellar, S. A. Ayaz, J. Laurie, J. Esterle, J. L. Crowley, G. Wood, and S. Bodorkos (2015), CA-IDTIMS dating of tuffs, calibration of palynostratigraphy and stratigraphy of the Bowen and Galilee basins, in *Bowen Basin Symposium 2015*, edited by J. W. Beeston, 211–218, Coal Geol. Group, Geol. Soc. of Australia, Brisbane, Australia.
Nutman, A. P., S. Buckman, H. Hidaka, T. Kamiichi, E. Belousova, and J. Aitchison (2013), Middle Carboniferous-Early Triassic eclogite–blueschist blocks within a serpentinite mélange at Port Macquarie, eastern Australia: Implications for the evolution of Gondwana's eastern margin, *Gondwana Res.*, *24*(3–4), 1038–1050.
Offler, R., and D. A. Foster (2008), Timing and development of oroclines in the southern New England Orogen, New South Wales, *Aust. J. Earth Sci.*, *55*(3), 331–340.
Pankhurst, R. J., C. W. Rapela, C. M. Fanning, and M. Márquez (2006), Gondwanide continental collision and the origin of Patagonia, *Earth Sci. Rev.*, *76*(3–4), 235–257.
Paterson, M., and L. Weiss (1966), Experimental deformation and folding in phyllite, *Geol. Soc. Am. Bull.*, *77*(4), 343–374.
Phillips, G., J. Robinson, R. Glen, and J. Roberts (2016), Structural inversion of the Tamworth Belt: Insights into the development of orogenic curvature in the southern New England Orogen, Australia, *J. Struct. Geol.*, *86*, 224–240.
Pisarevsky, S. A., G. Rosenbaum, U. Shaanan, D. Hoy, F. Speranza, and T. Mochales (2016), Paleomagnetic and geochronological study of carboniferous forearc basin rocks in the southern New England Orogen (eastern Australia), *Tectonophysics*, *681*, 263–277.

Price, P. L. (1997), Permian to Jurassic palynostratigraphic nomenclature of the Bowen and Surat Basins, in *The Surat and Bowen Basins, south-east Queensland*, edited by P. M. E. Green, pp. 137–178, Queensland Department of Mines and Energy, Brisbane, Australia.
Purdy, D., A. Cross, and P. Jell (2013), Triassic volcanic rocks (Chapter 5.13. 5), in *Geology of Queensland*, edited by P. Jell, pp. 433–444, Geol. Surv. of Queensland, Brisbane, Australia.
Retallack, G. J., P. R. Renne, and D. L. Kimbrough (1993), New radiometric ages for Triassic floras of southeast Gondwana, in *The Non-Marine Triassic*, edited by S. G. Lucas and M. Morales, pp. 415–418, New Mexico Museum of Nat.l Hist. and Sci., Albuquerque, New Mexico.
Riley, T. R., M. J. Flowerdew, and M. J. Whitehouse (2012), U–Pb ion-microprobe zircon geochronology from the basement inliers of eastern Graham Land, Antarctic Peninsula, *J. Geol. Soc.*, *169*(4), 381–393.
Rosenbaum, G., and W. Mo (2011), Tectonic and magmatic responses to the subduction of high bathymetric relief, *Gondwana Res.*, *19*(3), 571–582.
Runnegar, B., and J. A. Ferguson (1969), *Stratigraphy of the Permian and Lower Triassic Marine Sediments of the Gympie District*, 247–281 pp., Univ. of Queensland Press, Brisbane, Queensland.
Scheibner, E. (1996), *Geology of New South Wales—Synthesis*. Vol. 1 Structural Framework, 295 pp., Dept. of Miner. Resour., Geol. Surv. of New South Wales, Sydney.
Shaanan, U., G. Rosenbaum, P. F. Li, and P. M. Vasconcelos (2014), Structural evolution of the early Permian Nambucca Block (New England Orogen, eastern Australia) and implications for oroclinal bending, *Tectonics*, *33*, 1425–1443, doi:10.1002/2013TC003426.
Shaanan, U., G. Rosenbaum, S. A. Pisarevsky, and F. Speranza (2015), Paleomagnetic data from the New England Orogen (eastern Australia) and implications for oroclinal bending, *Tectonophysics*, *664*, 182–190.
Silver, P. G., R. M. Russo, and C. Lithgow-Bertelloni (1998), Coupling of South American and African Plate motion and plate deformation, *Science*, *279*(5347), 60–63.
Sivell, W. J., and M. T. McCulloch (2001), Geochemical and Nd-isotopic systematics of the Permo-Triassic Gympie Group, southeast Queensland, *Aust. J. Earth Sci.*, *48*(3), 377–393.
Sivell, W. J., and J. B. Waterhouse (1988), Petrogenesis of Gympie Group volcanics: Evidence for remnants of an early Permian volcanic arc in eastern Australia, *Lithos*, *21*(2), 81–95.
Sliwa, R. (1995), Regional structural geology of the central north D'Aguilar block, southeast Queensland, 296 pp., The Univ. of Queensland.
Stidolph, P., J. Dugdale, and F. E. Von Gneilinski (2016), Queensland Geological Record 2016/05: Stratigraphy, structure and gold mineralisation in the Gympie Group at Gympie, Queensland, *Rep. No. 99245*, 103 pp., Geol. Surv. of Queensland, Brisbane, Australia.
Sobolev, S. V., and A. Y. Babeyko (2005), What drives orogeny in the Andes?, *Geology*, *33*(8), 617–620.
Tang, E. H. J. (2004), *The Petrogenesis of the Station Creek Igneous Complex and Associated Volcanics, Northern New England Orogen*, 334 pp., Queensland Univ. of Technol., Brisbane, QLD.
Totterdell, J. M., J. Moloney, R. J. Korsch, and A. A. Krassay (2009), Sequence stratigraphy of the Bowen–Gunnedah and Surat Basins in New South Wales, *Aust. J. Earth Sci.*, *56*(3), 433–459.
Trouw, R. A. J., and M. J. De Wit (1999), Relation between the Gondwanide Orogen and contemporaneous intracratonic deformation, *J. Afr. Earth Sci.*, *28*(1), 203–213.
Vaughan, A. P. M., and R. J. Pankhurst (2008), Tectonic overview of the west Gondwana margin, *Gondwana Res.*, *13*(2), 150–162.
Veevers, J. J. (1989), Middle/Late Triassic (230±5 Ma) singularity in the stratigraphic and magmatic history of the Pangean heat anomaly, *Geology*, *17*(9), 784–787.
Veevers, J. J. (2004), Gondwanaland from 650–500 Ma assembly through 320 Ma merger in Pangea to 185–100 Ma breakup: Supercontinental tectonics via stratigraphy and radiometric dating, *Earth Sci. Rev.*, *68*(1–2), 1–132.
Veevers, J. J. (2013), Pangea: Geochronological correlation of successive environmental and strati-tectonic phases in Europe and Australia, *Earth Sci. Rev.*, *127*, 48–95.
Veevers, J. J., and P. Morgan (2000), *Billion-Year Earth History of Australia and Neighbours in Gondwanaland*, 400 pp., Gemoc Press, Newcastle, Australia.
Wartenberg, W., R. J. Korsch, and A. Schäfer (2003), The Tamworth Belt in southern Queensland, Australia: Thrust-characterized geometry concealed by Surat Basin sediments, *Geol. Soc. London, Spec. Publ.*, *208*(1), 185–203.
Waschbusch, P., R. J. Korsch, and C. Beaumont (2009), Geodynamic modelling of aspects of the Bowen, Gunnedah, Surat and Eromanga Basins from the perspective of convergent margin processes, *Aust. J. Earth Sci.*, *56*(3), 309–334.
Waterhouse, J. B., and P. E. Balfe (1987), Stratigraphic and faunal subdivision of the Permian rocks at Gympie, in *Field Conference Gympie District*, edited by C. Murray and J. B. Waterhouse, pp. 20–33, Geol. Soc. of Australia, Brisbane.
Waterhouse, J. B., and W. J. Sivell (1987), Permian evidence for trans-Tasman relationships between East Australia, New Caledonia and New Zealand, *Tectonophysics*, *142*(2–4), 227–240.
Webb, A. W., and I. McDougall (1967), Isotopic dating evidence on the age of the upper permian and middle triassic, *Earth Planet. Sci. Lett.*, *2*(5), 483–488.
Weiss, L. E. (1980), Nucleation and growth of kink bands, *Tectonophysics*, *65*(1), 1–38.
Woodward, N. B. (1995), Thrust systems in the Tamworth Zone, southern New England Orogen, New South Wales, *Aust. J. Earth Sci.*, *42*(2), 107–117.
Yan, J., P. G. Lennox, and R. Offler (2016), History of faulting in the Northern Hastings Block, southern New England Orogen, *Aust. J. Earth Sci.*, *63*(7), 821–841.